

PNNL-32103 Rev 0
DVZ-RPT-075 Rev 0

Evaluation of a Potential Groundwater Tracer Test in the Ringold Upper Mud Aquifer at the 100-H Area of the Hanford Site

September 2021

Rob D. Mackley
Josh Torgeson
Judy Robinson
Nik Qafoku
Mark Rockhold
Jon Thomle

DISCLAIMER

This report was prepared as an account of work sponsored by an agency of the United States Government. Neither the United States Government nor any agency thereof, nor Battelle Memorial Institute, nor any of their employees, makes **any warranty, express or implied, or assumes any legal liability or responsibility for the accuracy, completeness, or usefulness of any information, apparatus, product, or process disclosed, or represents that its use would not infringe privately owned rights.** Reference herein to any specific commercial product, process, or service by trade name, trademark, manufacturer, or otherwise does not necessarily constitute or imply its endorsement, recommendation, or favoring by the United States Government or any agency thereof, or Battelle Memorial Institute. The views and opinions of authors expressed herein do not necessarily state or reflect those of the United States Government or any agency thereof.

PACIFIC NORTHWEST NATIONAL LABORATORY
operated by
BATTELLE
for the
UNITED STATES DEPARTMENT OF ENERGY
under Contract DE-AC05-76RL01830

Printed in the United States of America

Available to DOE and DOE contractors from the
Office of Scientific and Technical Information,
P.O. Box 62, Oak Ridge, TN 37831-0062;
ph: (865) 576-8401
fax: (865) 576-5728
email: reports@adonis.osti.gov

Available to the public from the National Technical Information Service
5301 Shawnee Rd., Alexandria, VA 22312
ph: (800) 553-NTIS (6847)
email: orders@ntis.gov <<https://www.ntis.gov/about>>
Online ordering: <http://www.ntis.gov>

Evaluation of a Potential Groundwater Tracer Test in the Ringold Upper Mud Aquifer at the 100-H Area of the Hanford Site

September 2021

Rob D. Mackley
Josh Torgeson
Judy Robinson
Nik Qafoku
Mark Rockhold
Jon Thomle

Prepared for
the U.S. Department of Energy
under Contract DEAC0576RL01830

Pacific Northwest National Laboratory
Richland, Washington 99354

Summary

This document presents an evaluation of a potential groundwater tracer test in the uppermost RUM (Ringold Formation member of Wooded Island – upper mud unit) aquifer in the 100-H Area of the Hanford Site. The results from field electrical resistivity tomography (ERT) investigations, numerical flow and transport (F&T) modeling, coupled ERT-F&T model simulations, and laboratory resin experiments provide the technical basis for evaluating tracer test scenarios that minimize impacts to the 100-HX pump and treat (HX P&T) operations, and maximize hydrologic data acquisitions including the use of advanced surface geophysical techniques for monitoring tracer transport.

A convergent flow tracer test, where a tracer injection occurs at one well and the tracer migrates toward an extraction well, was selected for evaluation since it can be performed with minimal impact to P&T operations and remedial performance. Scenarios were evaluated for a pulsed tracer injection at varying concentrations and volumes in well 199-H3-13, located within the hydraulic capture zone of existing P&T extraction well 199-H3-22. The selection of this well allows for HX P&T extraction wells to continue operating during tracer testing activities.

Site-specific groundwater F&T simulations of the injection, transport, and capture of a bromide tracer were performed over a range of KBr injection concentrations (10 to 100 g/L) and volumes (10,000 and 50,000 gallons). Simulations predicted that peak tracer concentrations will occur in extraction well 199-H3-22 about ~100 days after injection and return to near-zero concentrations after ~150 days for all scenarios. Extracted concentrations are ~100 and 30 times lower than the injection concentration for injections of 10,000 and 50,000 gallons, respectively. Additional dilution of the tracer is expected (factor of 15) to occur due to blending with influent groundwater from other HX P&T extraction wells. Accordingly, bromide concentrations predicted in the HX P&T system range from ~0.01 to 1 g/L for the 10,000-gallon scenarios.

The potential for bromide to interfere with the removal of hexavalent chromium (Cr(VI)) with the SIR-700 ion exchange resin in the HX P&T was also evaluated with a series of laboratory batch and 1D flow column experiments. The SIR-700 resin was exposed to bromide concentrations ranging from 0.1 to 30 g/L, identifying no impact to Cr(VI) removal performance for bromide concentrations ≤ 1 g/L. Results also indicated that the release of bromide retained on the resin following the peak tracer arrival will not result in a high-concentration pulse of bromide into the P&T effluent stream. Experimental tests suggested that no difference in influent and effluent concentrations of bromide are expected during a potential tracer test where influent concentrations of bromide are ≤ 1 g/L.

ERT was also evaluated for monitoring tracer transport from the injection to extraction well. Results from the numerical F&T model were incorporated into subsequent ERT imaging simulations to evaluate the ability of ERT to monitor tracer transport. Results suggested that time-lapse ERT can spatially resolve the tracer location during transport from the injection well to the extraction well if water volumes are large and bromide concentrations are sufficiently high (e.g., 30 g/L).

Given the potential for high bromide concentrations to interfere with the resin performance, a tracer test involving an injection of 10,000 gallons of 10 g/L bromide solution into well 199-H3-13 is recommended, with subsequent capture of the tracer using extraction well 199-H3-22. At this injection concentration, bromide concentrations in the HX P&T are expected to be < 10 mg/L, with no expected performance impact to the SIR-700 resin for Cr(VI) removal. Although simulation results suggested that ERT imaging may be limited in its ability to spatially resolve tracer transport at a lower injection volume and concentration, it is plausible that field surveys may perform better than predicted by simulation. Hence, the use of ERT is recommended as it can provide another line of evidence in the quantitative tracer test

analysis, with minimal cost and schedule impacts associated with an autonomous ERT survey. In this way, more than one line of evidence can be used to characterize the RUM, which in turn will support optimizing P&T operations at 100-H.

Acknowledgments

We thank the entire 100-HR-3 project team and P&T operations staff at CPCCo for their support and collaboration (listed alphabetically): Ella Feist, Randal Fox, Travis Hammond, Avrom HaWaaboo, Jason Hulstrom, Emily McDonald, Dean Neshem, Darrell Newcomer, and Sarah Springer. We would also like to thank the following DOE-RL staff for their input and direction: Steve Balone, and Jason Capron, Ellwood Glossbrenner, and John Virgin.

We acknowledge and appreciate Brent Hicks for quality assurance support and Matt Wilburn for editorial assistance. We thank Vicky Freedman for her technical review of this report.

This document was prepared by the Deep Vadose Zone – Applied Field Research Initiative at Pacific Northwest National Laboratory. Funding was provided by the U.S. Department of Energy (DOE) Richland Operations Office. Pacific Northwest National Laboratory is operated by Battelle Memorial Institute for the DOE under Contract DE-AC05-76RL01830.

Acronyms and Abbreviations

CPCCo	Central Plateau Cleanup Company
DDI	double deionized
EC	electrical conductivity
ERT	electrical resistivity tomography
F&T	flow and transport
Hf	Hanford formation
IX	ion exchange
NQAP	Nuclear Quality Assurance Program
OU	operable unit
P&T	pump and treat
PNNL	Pacific Northwest National Laboratory
RD/RA WP	<i>100-HR-3 Remedial Design/Remedial Action Work Plan</i> RUM Ringold Formation member of Wooded Island – upper mud unit
Rwie	Ringold Formation member of Wooded Island – unit E
SGW	simulated groundwater

Contents

Summary	ii
Acknowledgments.....	iv
Acronyms and Abbreviations	v
Contents	vi
1.0 Introduction.....	1.1
1.1 Document Scope.....	1.1
1.2 Document Organization.....	1.2
2.0 Background.....	2.1
2.1 100-H Area Hydrogeology	2.1
2.2 Study Area Setting: HX P&T System and Well Network	2.2
2.3 Groundwater Tracer Testing.....	2.5
2.4 Evaluation Priorities and Test Design Considerations.....	2.6
2.5 Technical Evaluation Approach.....	2.7
3.0 ERT Site Characterization	3.1
3.1 Methods	3.1
3.2 Site Locations and Details	3.2
3.3 Results of 100-H ERT Imaging	3.3
4.0 Groundwater F&T Modeling Evaluation.....	4.1
4.1 Model Description	4.1
4.2 Simulation Results	4.3
5.0 Coupled F&T Model and Time-Lapse ERT	5.1
5.1 Methodology.....	5.1
5.2 Results.....	5.2
6.0 Blended Bromide Concentrations in HX P&T System.....	6.1
7.0 Laboratory Evaluations of Bromide and SIR-700 Resin	7.1
7.1 Batch Tests.....	7.1
7.2 Column Tests	7.2
7.2.1 Methodology.....	7.2
7.2.2 Br Results	7.3
7.2.3 Cr Results	7.6
8.0 Integrated Evaluation Discussion and Conclusions.....	8.1
8.1 Outcome and Remedial Impact.....	8.1
8.2 Compatibility with HX P&T System.....	8.1
8.2.1 Operational Impacts.....	8.2
8.2.2 SIR-700 Resin Performance Impacts	8.2
8.2.3 Effluent Bromide Concentrations.....	8.2
8.3 Tracer ERT Monitoring	8.3

8.3.1 Site-Specific ERT Characterization..... 8.3
8.3.2 Tracer Concentration and Volume Requirements 8.3
8.3.3 Transport Estimates 8.3
8.3.4 Recommended ERT Collection..... 8.3
9.0 Conceptual Tracer Test Design..... 9.1
10.0 Quality Assurance..... 10.1
11.0 References..... 11.1
Appendix A – Laboratory Batch Tests A.1

Figures

Figure 1.1.	Map showing the 100-HR-3 Groundwater Operable Unit.....	1.3
Figure 1.2.	Map showing the Cr(VI) plumes in the Horn and 100-H areas within the uppermost RUM aquifer	1.4
Figure 2.1.	Conceptualized hydrogeology for the 100-HR-3 OU (from DOE/RL-2019-66, Rev. 0).....	2.2
Figure 2.2.	Map showing the network of wells connected to the 100 DX and 100 HX P&T facilities within the 100-HR-3 Groundwater Operable Unit (from DOE/RL-2019-67, Rev. 0; Figure 1-2).....	2.4
Figure 2.3.	Map showing the location of RUM aquifer wells within the 100-H tracer test study area.	2.5
Figure 3.1.	Area of ERT evaluation within 100-H showing electrode locations	3.2
Figure 3.2.	Figures showing the layout of ERT line 1	3.4
Figure 3.3.	ERT images for lines 1b and 2 and Washington State Plane coordinates	3.6
Figure 4.1.	Modeled domain showing selected hydrogeologic units at the 100-H Area	4.2
Figure 4.2.	Modeled domain showing selected hydrogeologic units at the 100-H Area	4.5
Figure 5.1.	Schematic depicting coupled F&T and time-lapse ERT simulations to evaluate ERT feasibility to monitor a tracer injection.	5.2
Figure 5.2.	Time-lapse images showing true bulk EC from the F&T simulations and ERT bulk EC	5.4
Figure 5.3.	Spatial moment analysis comparing center-of-mass estimates for tracer concentrations	5.5
Figure 5.4.	Time-lapse images showing true bulk EC from the F&T simulations and ERT bulk EC	5.6
Figure 7.1.	Column 1 influent Br concentration (light blue) and effluent Br concentration (dark blue) versus number of pore volumes.	7.4
Figure 7.2.	Column 2 influent Br concentration (light blue) and effluent Br concentration (dark blue) versus number of pore volumes.	7.5
Figure 7.3.	Column 3 influent Br concentration (light blue) and effluent Br concentration (dark blue) versus number of pore volumes.	7.5
Figure 7.4.	Concentrations of column 3 influent sulfate (yellow dotted line), effluent sulfate (yellow solid line), and effluent bromide (blue) versus number of pore volumes.	7.6
Figure 7.5.	Column 1 influent chromate concentration (light orange) and effluent chromate (dark orange) versus number of pore volumes.....	7.7
Figure 7.6.	Column 2 influent chromate concentration (light orange) and effluent chromate (red) versus number of pore volumes.	7.7
Figure 7.7.	Column 3 influent chromate (orange) and effluent chromate (dark orange) versus number of pore volumes.	7.8

Tables

Table 2.1.	Aquifer hydraulic property estimates for the uppermost RUM aquifer in the 100-H Area (from Mackley et al. 2020).....	2.2
Table 2.2.	Technical approach for evaluating a potential tracer test in the RUM aquifer in the 100-H study area.	2.7
Table 3.1.	100-H ERT line details.	3.3
Table 4.1.	Parameters used in F&T modeling to represent hydrogeologic units (HGU) in the 100-H tracer test study area.	4.3
Table 4.2.	Modeling scenarios for injection of a KBr tracer into well 199-H3-13.	4.4
Table 6.1.	Predicted peak bromide concentrations in extraction well 199-H3-22 and the HX P&T system for a range of tracer concentrations and volumes.	6.1
Table 7.1.	Bromide and chromate concentrations used in column tests.	7.2
Table 9.1.	Conceptual tracer design recommendations for a potential bromide tracer test in the uppermost RUM aquifer in the 100-H Area	9.1

1.0 Introduction

Past operations in the 100-HR-3 Operable Unit (OU), located in the north-central part of the Hanford Site (Figure 1.1), have resulted in the contamination of soil and groundwater with Cr(VI). Dissolved Cr(VI) in groundwater is distributed as broad plumes within the overlying unconfined and RUM (Ringold Formation member of Wooded Island – upper mud unit) aquifers (DOE/RL-2010-95, Rev. 0). Decades of groundwater pump and treat (P&T) aquifers and excavation of contaminated soil have reduced concentrations in groundwater and decreased the areal extent of plumes within the unconfined aquifer. However, high Cr(VI) concentrations ($>100 \mu\text{g/L}$) continue to persist above target cleanup levels ($48 \mu\text{g/L}$) in the underlying RUM aquifer in the Horn (area between 100-D and 100-H) and 100-H areas (Figure 1.2).

There is a need to better understand the hydrologic and contaminant transport properties of the RUM aquifer in order to optimize removal of Cr(VI). The highest concentrations of Cr(VI) in the 100-HR-3 OU are found in this deeper, semi-confined RUM aquifer (DOE/RL-2019-66, Rev. 0). The *100-HR-3 Remedial Design/Remedial Action Work Plan* (RD/RA WP; DOE/RL-2017-13, Rev. 0) identified the need for a more quantitative understanding of the groundwater flow and Cr(VI) transport behavior of the RUM aquifer. To this end, a multi-year hydrologic characterization for the RUM aquifer was initiated in FY19. A series of hydrologic characterization activities were performed and analyzed in FY19 and FY20 to provide the spatial distribution of aquifer hydraulic properties (e.g., hydraulic conductivity and the vertical leakage) for the RUM aquifer throughout the 100-H Area, where Cr(VI) concentrations in the RUM are the highest (Mackley et al. 2020).

Groundwater tracer testing was explicitly identified as one of the key activities for characterizing the RUM aquifer in the RD/RA WP (DOE/RL-2017-13, Rev 0). Groundwater tracer tests are a widely used investigation method for measuring groundwater flow velocity and direction, aquifer hydraulic properties, and transport processes. Additionally, when performed in active groundwater P&T systems, groundwater tracers can help determine the remedial impact and radial extent of hydraulic capture zones or flow-path control exerted by operating extraction wells, which in turn determines the number of wells, cost, and timeframe required to meet cleanup goals (Cohen et al. 1994; Kim 2014).

During FY21, an in-depth and integrated technical evaluation of a potential tracer test within the 100-H area in the RUM aquifer was performed to provide the basis for determining the technical feasibility, implementability, expected outcome, and associated performance monitoring approach (including the use of geophysics). Hydrologic characterization of the RUM aquifer from a potential tracer test will help form the basis for improved decisions for P&T remediation of Cr(VI) within the RUM aquifer. Performing a groundwater tracer test within a network extraction and wells connected to an active P&T system provides a suite of unique challenges and opportunities and these need to be evaluated prior to implementation.

1.1 Document Scope

This document presents the integrated results of a technical feasibility evaluation for a variety of tracer testing scenarios in the RUM aquifer in the 100-H Area. It forms the technical basis for selecting a suitable tracer test design and decision to proceed with field implementation. Results from field investigations, numerical modeling simulations, and laboratory experiments are presented. The expected test outcomes in relation to information needs for the RUM aquifer were considered for a variety of ionic tracer test scenarios (i.e., concentration, volume, duration, and well locations).

The tracer test scenarios evaluated in this document reflect test objectives identified in the 100-HR-3 RD/RA WP (DOE/RL-2017-13, Rev 0), remedial operational priorities for the 100 HX P&T (herein HX P&T) system, and conceptual understanding of the RUM aquifer in the 100-H study area. The final test design parameters and key activities involving coordination and support by the site contractor will need to be documented in subsequent field test procedures and instructions, once the determination to proceed with field implementation has been made.

1.2 Document Organization

Following the introduction of this report, Section 2.0 contains background information, including the hydrogeology of the 100-H tracer test study area, a summary of the HX P&T system and well network, information on groundwater tracer testing, the key priority and design considerations in the technical evaluations, and a summary of the evaluation approach. Section 3.0 presents the methods and results of an electrical resistivity tomography (ERT) field characterization of the study area. The methods and results of the site-specific RUM aquifer groundwater flow and transport (F&T) model simulations of varying bromide (Br) tracer test scenarios are given in Section 4.0. Section 5.0 contains the methods and results of ERT imaging simulations incorporating the site-specific numerical F&T model simulations for the tracer test scenarios. Section 6.0 presents blended Br tracer concentrations predicted in the HX P&T system based on the F&T modeling results. The methods and results of a series of laboratory experiments evaluating effects of Br on the Cr(VI) removal performance of the SIR-700 resin used in the HX P&T system are presented in Section 7.0. Section 8.0 provides an integrated discussion and conclusions from the technical evaluation, followed by the conceptual design for a potential tracer test in the uppermost RUM aquifer in the 100-H study area in Section 9.0. Supplemental information on the laboratory batch experiments is provided in Appendix A.

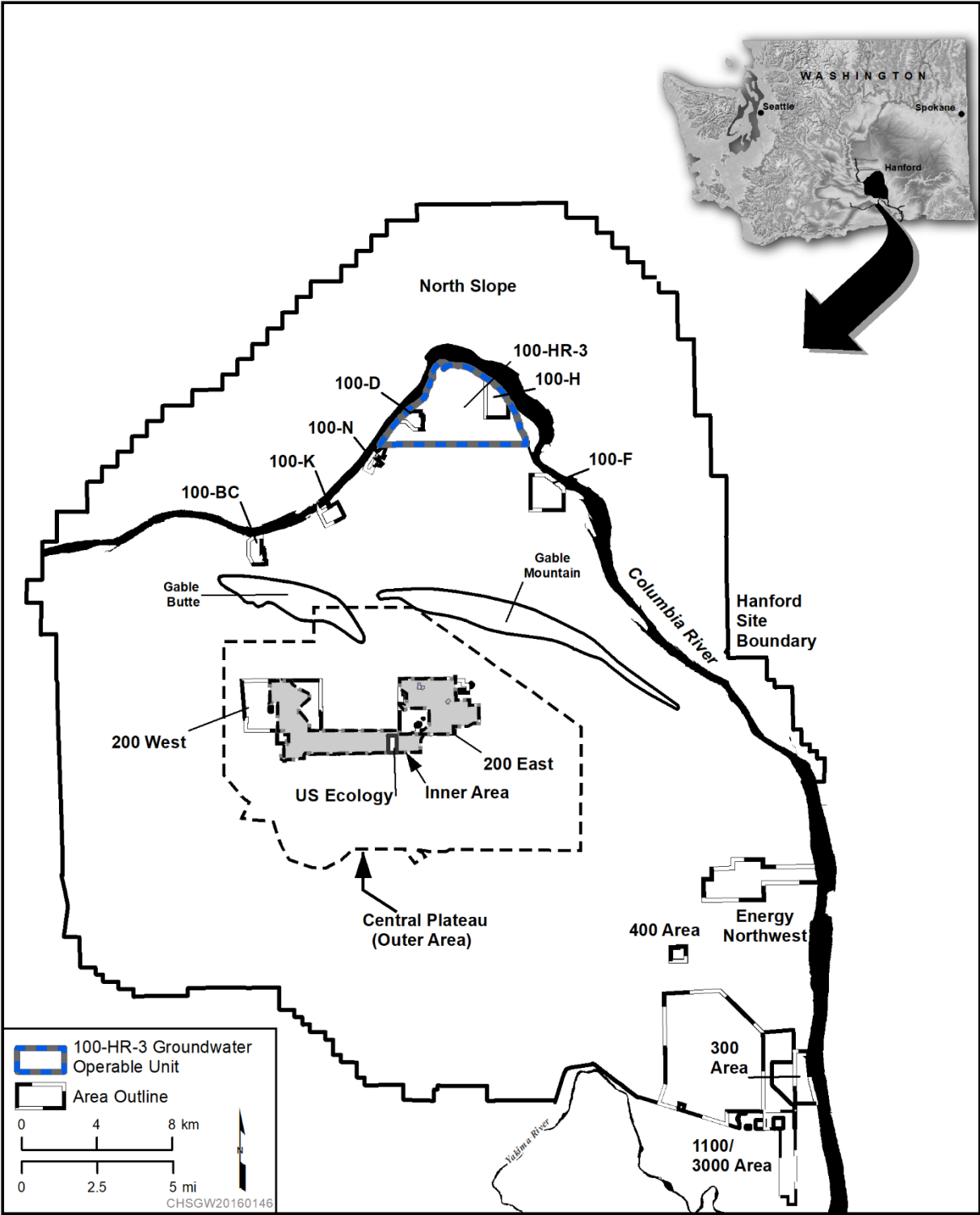


Figure 1.1. Map showing the 100-HR-3 Groundwater Operable Unit located within the northwest region of the Hanford Site (from SGW-60571, Rev. 0).

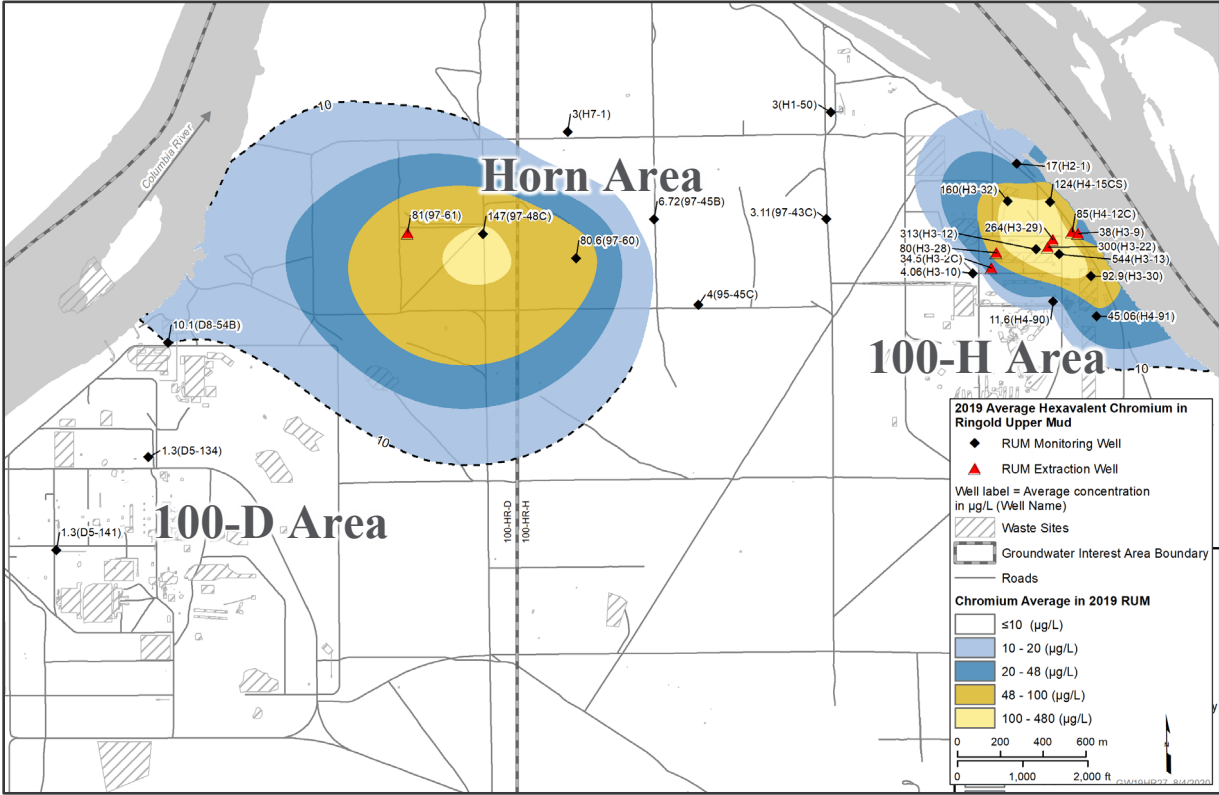


Figure 1.2. Map showing the Cr(VI) plumes in the Horn and 100-H areas within the uppermost RUM aquifer, which continue to persist above the 48 µg/L cleanup level (modified from DOE/RL-2019-66, Rev. 0).

2.0 Background

This section provides a summary of the hydrogeology of the 100-H study area and the HX P&T system associated well network, and information on groundwater tracer studies as they relate to characterization of the RUM aquifer within the 100-H study area.

2.1 100-H Area Hydrogeology

The three hydrogeologic units of interest within the 100-H study area are the Hanford formation (Hf), the Ringold Formation member of Wooded Island – unit E (Rwie), and the RUM (Figure 2.1). Material of the Hf (an informal geologic unit) consists predominantly of unconsolidated sediments that cover a wide range of grain sizes, from boulder-sized gravel to sand, silty sand, and silt. The unconfined aquifer at 100-H is primarily within the gravel-dominated Hf, although there are localized areas where the Rwie is present and underlies the Hf (DOE/RL-2010-95, Rev. 0). The Rwie unit consists of a fluvial matrix supported by gravels and sands with intercalated fine- to coarse-grained sand and silt layers and is relatively less transmissive than the overlying Hf (SGW-60571).

RUM sediments are relatively lower in permeability and form the base of the unconfined aquifer in 100-H Area (Figure 2.1). The silt- and clay-laden RUM has lower hydraulic conductivity relative to the Hf and Rwie. The top of the RUM forms a confining layer or aquitard between the overlying unconfined aquifer and the uppermost RUM aquifer and varies in thickness from about 3 to 13 meters in the 100-H Area (Mackley et al. 2020). Below the fine-grained and low-permeability RUM confining layer is the uppermost RUM aquifer, also referred to as the first water-bearing unit in the RUM (DOE/RL-2010-95, Rev 0). The uppermost RUM aquifer consists of silty-sand layers. In the 100-H Area, it appears the uppermost RUM aquifer varies in thickness between about 6 and 14 meters (Mackley et al. 2020). Fine-grained silts and clays form the base of the uppermost RUM aquifer. Deeper transmissive water-bearing units can be found in the RUM (e.g., second and third water-bearing units of the RUM; DOE/RL-2010-95, Rev. 0). However, no Cr(VI) contamination has been found in the deeper water-bearing units, and it is highly uncertain if these deeper water-bearing units are laterally continuous and how they relate stratigraphically to other Ringold Formation units regionally (Mackley et al. 2020).

Mackley et al. (2020) provides a comprehensive review of historical hydrologic investigations in the RUM aquifer as well as new results from a series of aquifer tests. Results from multi-well pumping testing confirm the uppermost RUM aquifer is laterally connected at distances spanning 500 meters or more within the 100-H test area and is a semiconfined (leaky-confined) aquifer (Mackley et al. 2020). The aquifer hydraulic and storage properties for the uppermost RUM aquifer and the RUM overlying confining layer within the 100-H tracer test study area are summarized in Table 2.1.

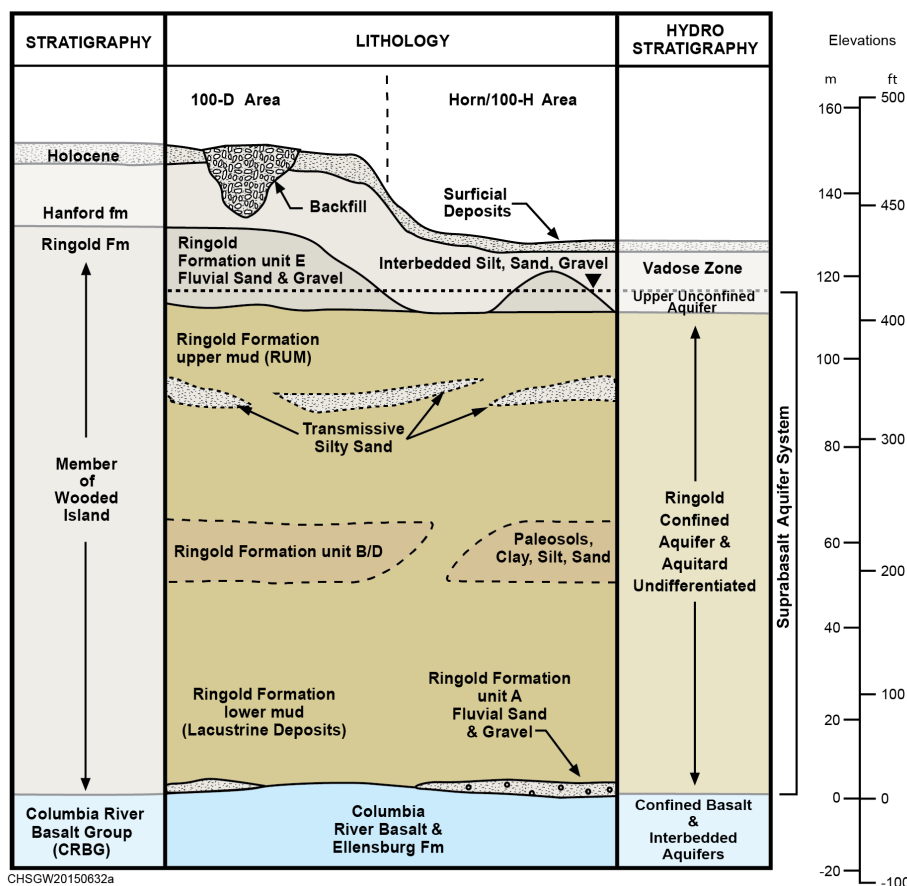


Figure 2.1. Conceptualized hydrogeology for the 100-HR-3 OU (from DOE/RL-2019-66, Rev. 0).

Table 2.1. Aquifer hydraulic property estimates for the uppermost RUM aquifer in the 100-H Area (from Mackley et al. 2020).

	Minimum ^(a)	Maximum	Geometric Mean
Transmissivity (T)	27.7m ² /day	236.8 m ² /day	83.3m ² /day
Hydraulic conductivity ^(b) (K)	2.8 m/day	24.2 m/day	8.5 m/day
Storativity (S)	1.4x10 ⁻⁴	1.3x10 ⁻³	3.4x10 ⁻⁴
Confining layer vertical hydraulic conductivity (K')	2.7x10 ⁻³ m/day	4.9x10 ⁻² m/day	1.3x10 ⁻² m/day

(a) Minimum, maximum, and geometric means from multiple pumping tests in the 100-H Area.

(b) $K = T/b$; where b = average aquifer thickness = 9.8 m (Mackley et al. 2020; Table 2.2).

2.2 Study Area Setting: HX P&T System and Well Network

The HX P&T facility, located in the 100-H Area, is one of two active P&T systems operating in the 100-HR-3 OU for removal of Cr(VI) in groundwater and has an associated network of extraction and injection wells (Figure 2.2). Currently, there are six RUM aquifer extraction wells connected to the HX P&T system (Figure 2.3). Two of these RUM extraction wells (199-H3-22 and 199-H3-29) are located within the center of the Cr(VI) plume (Figure 1.2 and Figure 2.3).

During calendar year 2019, a total of 30.6 kg of Cr(VI) was removed from the unconfined and RUM aquifers through extraction wells connected to the HX P&T facility (DOE/RL-2019-67, Rev. 0). A disproportionately large amount of the total mass treated through the HX P&T facility was from RUM aquifer extraction wells since most of these are located within the higher-concentration portion of the Cr(VI) plume in the RUM aquifer (Figure 1.2). This underscores the priority to minimize impacts or downtime to ongoing P&T operations and accompanying Cr(VI) mass removal during any potential hydraulic testing activities. Additionally, hydraulic interference (drawdown) by nearby extraction wells in the area could also complicate the implementation or interpretations of hydraulic testing activities. On the other hand, the presence of P&T extraction wells that are already connected to a groundwater treatment facility provides an opportunity for long-term pumping and extraction of a tracer without incurring costly and logistically complex purge water disposal normally associated with these types of tests.

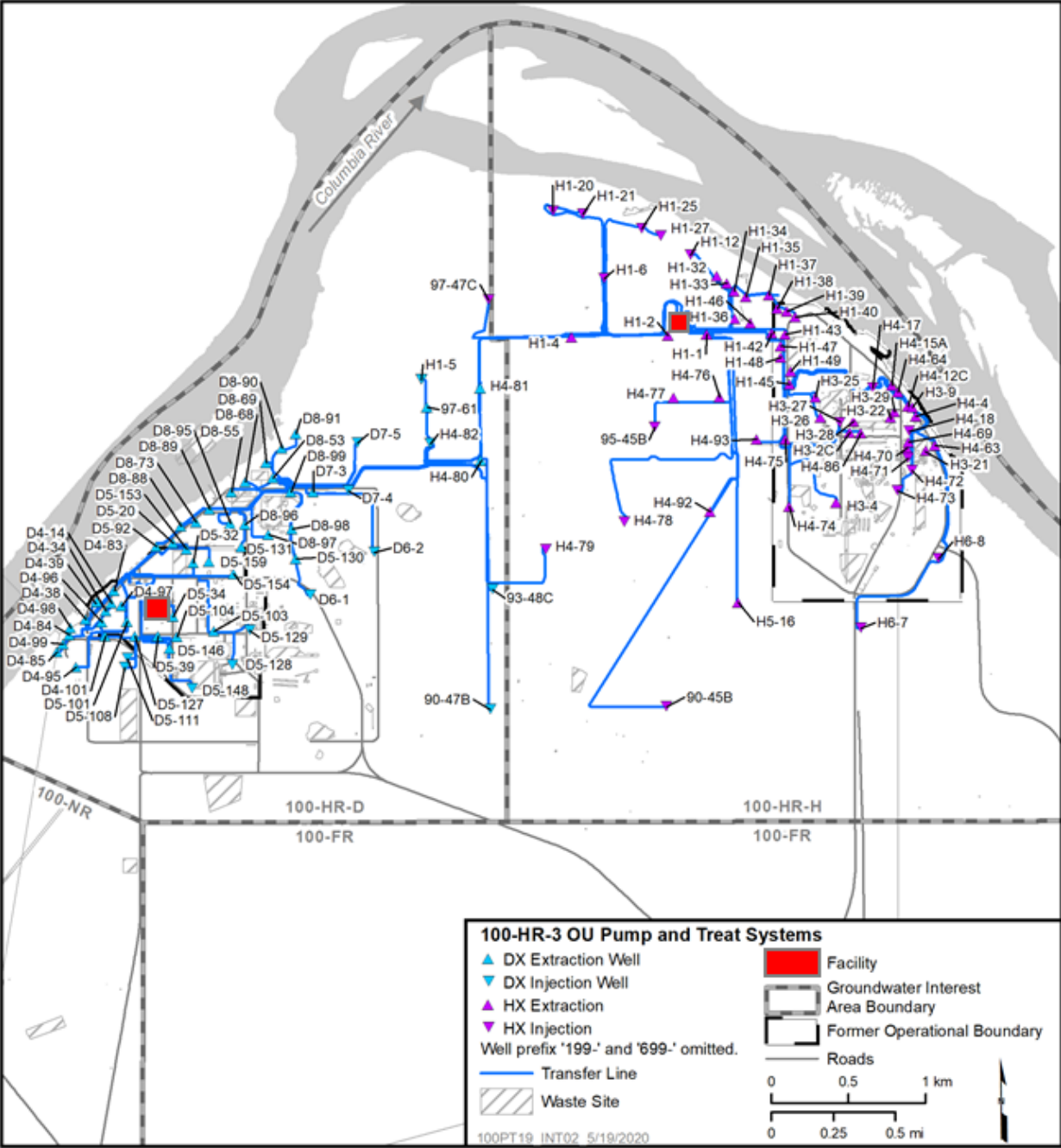


Figure 2.2. Map showing the network of wells connected to the 100 DX and 100 HX P&T facilities within the 100-HR-3 Groundwater Operable Unit (modified from DOE/RL-2019-67, Rev. 0; Figure 1-2).

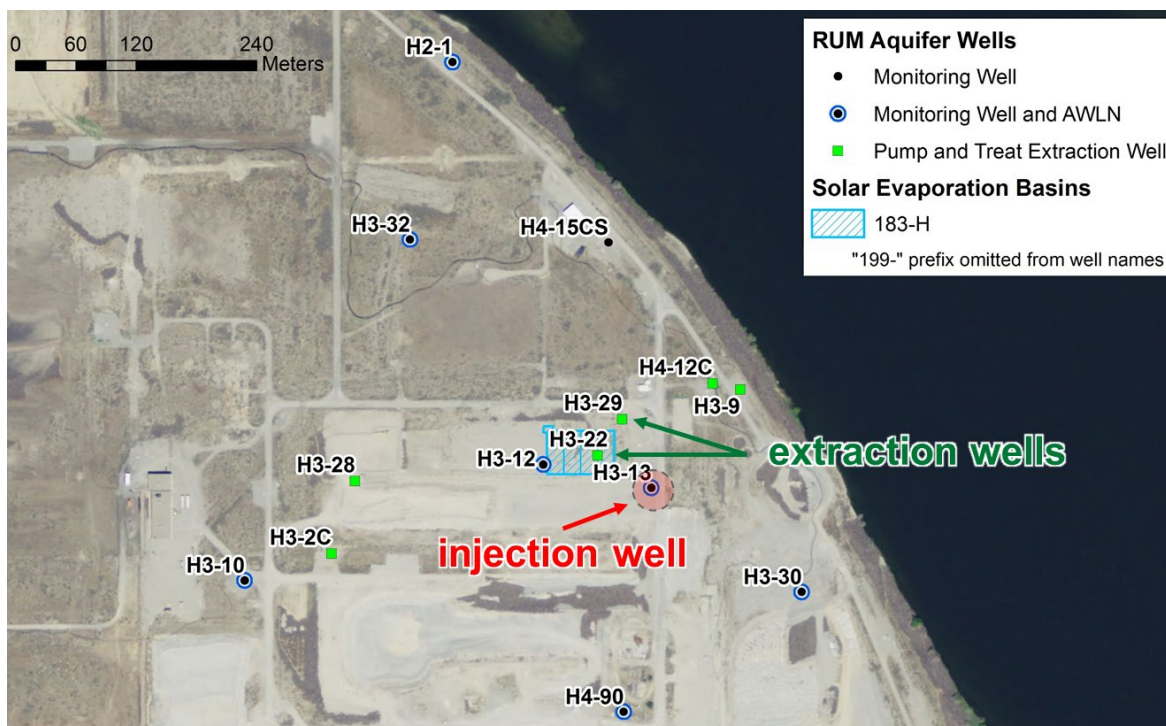


Figure 2.3. Map showing the location of RUM aquifer wells within the 100-H tracer test study area, including the proposed tracer injection and extraction wells.

2.3 Groundwater Tracer Testing

Groundwater tracer testing is a hydrologic investigation method for evaluating groundwater flow (velocity and direction), solute transport processes, and aquifer hydraulic properties. Tracer tests involve emplacing a chemical substance into the groundwater flow system via one or more wells. When a non-reactive (conservative) chemical tracer is emplaced, it is transported within the groundwater flow system through the processes of advection, dispersion, and diffusion.

Forced-gradient tracer tests involve the transport of an emplaced tracer under an induced groundwater flow field. Maliva (2016) provides a review of various types of forced-gradient tracer tests. One of these is the convergent flow tracer test, in which groundwater is pumped from one or more extraction wells until a steady-state flow field is established. Next, a tracer is emplaced in the aquifer through a pulsed injection into one or more wells and is transported along the groundwater flow path until being captured by one or more extraction wells. The arrival (breakthrough) curve characteristics in the extraction well(s) are monitored and analyzed to estimate the groundwater velocity, transport, and aquifer hydraulic properties.

When tracer tests are performed in settings with active groundwater P&T remedies, such as the 100-H study area, they can help determine the remedial impact and radial extent of hydraulic capture zones or flow-path control exerted by operating extraction wells, which in turn determines the number of wells, cost, and timeframe required to meet cleanup goals (Cohen et al. 1994; Kim 2014). Tracer testing was explicitly identified in the *Remedial Design/Remedial Action Work Plan for the 100-DR-1, 100-DR-2, 100-HR-1, 100-HR-2, and 100-HR-3 Operable Units* as a necessary and appropriate investigation method for the RUM aquifer (DOE/RL-2017-13, Rev. 0) and is being planned as one of the next steps in the multi-year hydrologic characterization effort for the RUM aquifer.

2.4 Evaluation Priorities and Test Design Considerations

Performing a groundwater tracer test within a network of P&T wells provides a suite of unique challenges and opportunities that were considered from the earliest stages of the evaluation. Selecting a test type, well configuration, and preliminary design for compatibility with the HX P&T system was prioritized in the initial test type and designs.

RUM aquifer characterization activities, such as the tracer testing presented here, are needed to understand the number and optimal locations of extraction wells and time needed to meet cleanup levels with the P&T remedy (DOE/RL-2017-13, Rev. 0). However, it is also important that a potential tracer test minimize impact to the ongoing P&T operations to maintain optimal remedial performance. For example, shutting down multiple P&T extraction wells in the RUM aquifer for extended time periods is not practical. This guided the initial selection of a tracer test that would minimize interruption to P&T operations.

As discussed in Section 2.3, a convergent flow tracer test involves injecting a tracer into the aquifer through an injection well, subsequent transport with groundwater along a forced-gradient flow field, and capture (recovery) through a continuously pumping extraction well. Monitoring well 199-H3-13, located within the high-concentration portion of the Cr(VI) plume (Figure 1.2 and Figure 2.3) can be used as the tracer injection well. Previous hydraulic testing estimated hydraulic conductivity (K) for the uppermost RUM aquifer within this zone of wells (Mackley et al. 2020). Testing also confirmed there is a direct hydraulic connection between well 199-H3-13 and other nearby RUM aquifer extraction wells such as 199-H3-22 and 199-H3-29, located approximately 63 and 75 meters away, respectively (Mackley et al. 2020). Well 199-H3-13 does not have a dedicated sampling pump permanently installed, which will allow physical access to the well during tracer testing without requiring pump removal/reinstallation. This type of tracer test allows P&T extraction wells to remain running (including 199-H3-22 and 199-H3-29) throughout all tracer testing activities. Downhole sensors capable of recording water-level, temperature, and specific conductance were already installed in these three wells to support previous RUM aquifer monitoring and hydraulic characterization (Mackley et al. 2020).

Selection of an appropriate tracer composition is a key component of test planning and design (Davis et al. 1980; Maliva 2016). Geophysical monitoring methods, such as ERT, have the potential to provide observations of tracer behavior between the injection and extraction wells that can be used to supplement extraction well breakthrough curves in the analysis of a tracer tests. This additional information can help improve estimates of the hydrologic properties that control flow and transport processes and thus improve flow and transport predictions (Dafflon et al. 2011). ERT monitoring of tracer transport requires a time-varying change in bulk electrical conductivity (EC), and this guided the initial selection for evaluating a tracer of ionic composition. Bromide and chloride based ionic tracers have been used extensively at Hanford for decades (Williams et al. 2000, 2008; Truex et al. 2009; Vermeul et al. 2013). They are generally inexpensive, easy to mix and inject in the field, provide non-reactive (conservative) transport, can be monitored in the field in real time using in situ sensors (e.g., ion selective electrodes or specific conductance probes), and analyzed in the laboratory using ion chromatography. However, effective imaging of a tracer test using ERT usually requires the use of high concentrations of ionic solutes to create large enough changes in EC for plumes to be imaged effectively (Robinson et al. 2020). This can be problematic since high concentrations can result in plume sinking behavior (density-driven flow) and high concentrations of KBr could interfere with the ability of the SIR-700 resin used in the HX P&T system to remove Cr(VI). Both issues will be considered as part of the technical evaluation.

As noted, a variety of ionic (bromide- and chloride-based solutions) tracers have been used at Hanford in the past. For the 100-H RUM aquifer tracer test evaluation, potassium bromide (KBr) was selected over

other options from the onset given (1) Br is less regulated for environmental permitting than chloride and (2) KBr has a higher electrolytic conductivity than NaBr (Isono 1984), and corresponding signal for ERT.

In summary, the tracer test type, well locations, and composition were selected up front in the evaluation given the priorities to (1) provide hydrologic information for the RUM aquifer and the P&T system needed for remedial decisions, (2) minimize or prevent impacts to P&T operations during tracer testing, and (3) utilize ERT as a method for monitoring transport processes in complex remedial settings such as the 100-H study area. Additional test and monitoring design specifications, such as the tracer volume and concentration and field monitoring approach, were further refined based on the integrated results of the technical evaluation.

2.5 Technical Evaluation Approach

Performing detailed “pre-field” technical evaluations (Robinson et al. 2020) and forward modeling using site-specific information (Maliva 2016) increases the likelihood for successful test outcomes. The results of this multidisciplinary technical evaluation provide the basis for determining feasibility, design (operations and monitoring), and realistic expectations for test outcomes relative to site-specific conditions and test objectives. Table 2.2 summarizes the site-specific technical elements, evaluation approach, and corresponding report sections for evaluating a potential tracer test in the RUM aquifer involving P&T wells in the 100-H study area.

Table 2.2. Technical approach for evaluating a potential tracer test in the RUM aquifer in the 100-H study area.

Evaluation Elements	Evaluation Approach	Report Section
Performance and design of ERT monitoring of tracer test in the RUM aquifer	1. Collect and evaluate site-specific bulk EC of the subsurface for the study area using a series of field ERT surveys.	Section 3.0
	2. Identify buried metallic infrastructure or other factors that may impact the performance of ERT imaging.	
	3. Select well location(s) within study area for potential tracer test to maximize ERT performance.	
	4. Simulate tracer transport within the RUM aquifer for a variety of tracer volumes and concentrations using a site-specific F&T model.	Section 4.0
	5. Simulate time-lapse ERT images of tracer transport at varying injection volumes and concentrations based on simulations from F&T model.	Section 5.0
	6. Compare predicted ERT images of tracer transport with simulations from F&T model.	
Potential tracer test impacts to P&T operations and Cr(VI) treatment	1. Select a tracer test type and configuration that is compatible with the HX P&T system and the existing network of wells, and that avoids shutdown of extraction wells and disruption to P&T operations.	Section 2.4
	2. Estimate tracer transport duration, concentration in extraction wells (breakthrough curve), blended tracer concentration in HX P&T system, and effluent concentration at varying tracer injection concentrations and volumes using F&T simulations.	Section 4.0
	3. Evaluate potential ionic tracer (KBr) impacts to SIR-700 treatment for Cr(VI) with laboratory experiments at varying Br tracer concentrations.	Section 7.0

3.0 ERT Site Characterization

Preliminary ERT site characterization allows for a better understanding of site-noise, EC range and magnitudes, and the depth of investigation. Site-specific ERT can also be used to evaluate tracer tests. ERT site characterization surveys were collected along 2D transects as part of the overall tracer feasibility evaluation. This section describes ERT and its uses, followed by a site description and application in the 100-H study area.

3.1 Methods

Electrical resistivity (the inverse of EC) quantifies how strongly a material opposes the flow of an electrical current. This is controlled by porosity, moisture content, temperature, pore water fluid conductivity, and soil texture. ERT is an active source geophysical method that uses an array of electrodes to image subsurface bulk EC. For a given measurement, two electrodes within the array are used to inject a direct-current into the subsurface and two other receiving electrodes are used to measure the voltage. The basic unit of ERT data is transfer resistance (ohm), which is the measured voltage drop (ΔV) across the receiving electrodes divided by the injected current (I).

This monitoring evaluation consisted of synthetic and field ERT data acquired from surface electrode arrays. In a field installation, surface arrays consist of electrodes, which are metal stakes hammered into the surface. The electrodes are then connected to a wire leading to a resistivity data collection instrument. Static ERT, referred to herein as ERT, is where an ERT dataset is collected at a single point in time and analyzed independently to produce an image of bulk EC. Time-lapse ERT simulations were used to evaluate the ability of ERT to monitor changes from a simulated tracer injection over time. Time-lapse ERT can be advantageous relative to ERT because the competing effects of lithology, porosity, and other factors can be eliminated by focusing on changes in bulk EC over time rather than on absolute bulk EC (Singha et al. 2015).

ERT imaging resolution is governed by many factors, including electrode spacing, proximity to electrodes, background electrical noise, and measurement sequence. Bulk EC distribution impacts imaging resolution as this controls how and where electrical current flows in the subsurface. For example, current will preferentially flow within a fine-grained (silt/clay) layer, and this can reduce the ability of ERT to image below this layer. In addition, resolution for surface measurements is highest closer to the surface where the electrodes are located and decreases with depth. Limited resolution effects are important to consider when interpreting ERT images. In particular, the spatial extents of bulk EC plumes are likely to appear larger in the ERT images than they are in reality, with the outer extents of plumes beyond the true extents. Small-scale features may also not be resolved and larger resolvable features will be manifest as smoothed or blurred versions of the actual subsurface bulk EC.

The open-source finite element code E4D was used for the ERT evaluations. E4D allows for a flexible set of inputs, including engineering information such as the location of metallic infrastructure, which can be used as constraints on the solution. The E4D mesh uses unstructured tetrahedral elements and users can place boundaries within the mesh and use those boundaries to add information to the inversion. This flexible formulation provides the ability to incorporate all available information, subject to data fit, resulting in improved imaging resolution and a physically realistic interpretation.

Buried metallic infrastructure, such as well casings, pipes, and concrete structures containing rebar, redistributes subsurface current flow during ERT measurements and can significantly impact resulting images (Johnson and Wellman 2013). If metallic subsurface features are not modeled correctly, anomalously high conductivity features will appear in the vicinity of the infrastructure to match the ERT measurements. Johnson and Wellman (2015) demonstrated a method of removing the effects of buried infrastructure by explicitly modeling the infrastructure in the forward modeling phase of the ERT imaging algorithm. This methodology is contained within the E4D Infrastructure Modeling and Inversion module. For this evaluation, if a high-conductivity anomaly appeared in the ERT images, an investigation was conducted to determine if metallic infrastructure was present, and if so, it was incorporated within the E4D modeling.

3.2 Site Locations and Details

ERT data was collected within the 100-H study area along three lines (Figure 3.1, Table 3.1) to evaluate data noise levels, site-specific bulk EC, and feasibility of monitoring a tracer injection. Line 1, consisting of 175 electrodes, was run from southwest to northeast across the former 183-H Solar Evaporation Basin with a line-length designed to image down to and/or below the RUM aquifer. Line 1b contained 64 electrodes on the northeastern side of line 1 and was positioned to avoid infrastructure effects observed in ERT images from line 1. To evaluate the feasibility of ERT for tracer monitoring, line 2 was subsequently installed to better align with the proposed tracer flow path running from the proposed injection well 199-H3-13 to extraction well 199-H3-22 and 199-H3-29. This allowed for a better understanding of geologic structure and impacts/locations of unknown metallic infrastructure. The ERT images from line 2 were also used in the coupled F&T and time-lapse ERT evaluation (Section 5.0).

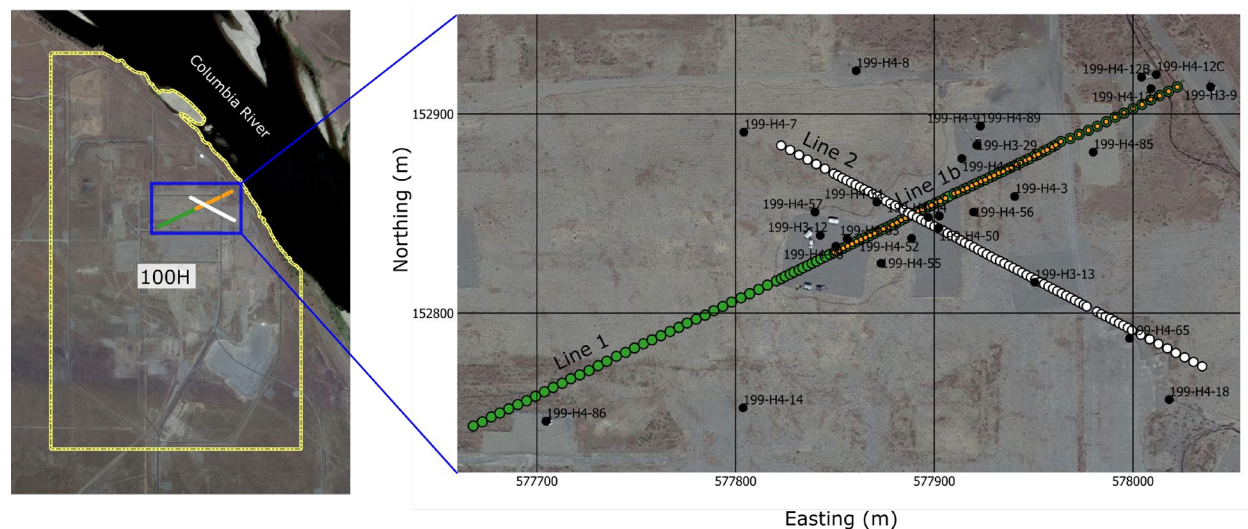


Figure 3.1. Area of ERT evaluation within 100-H showing electrode locations as green (line 1), orange (line 1b), and white circles (line 2).

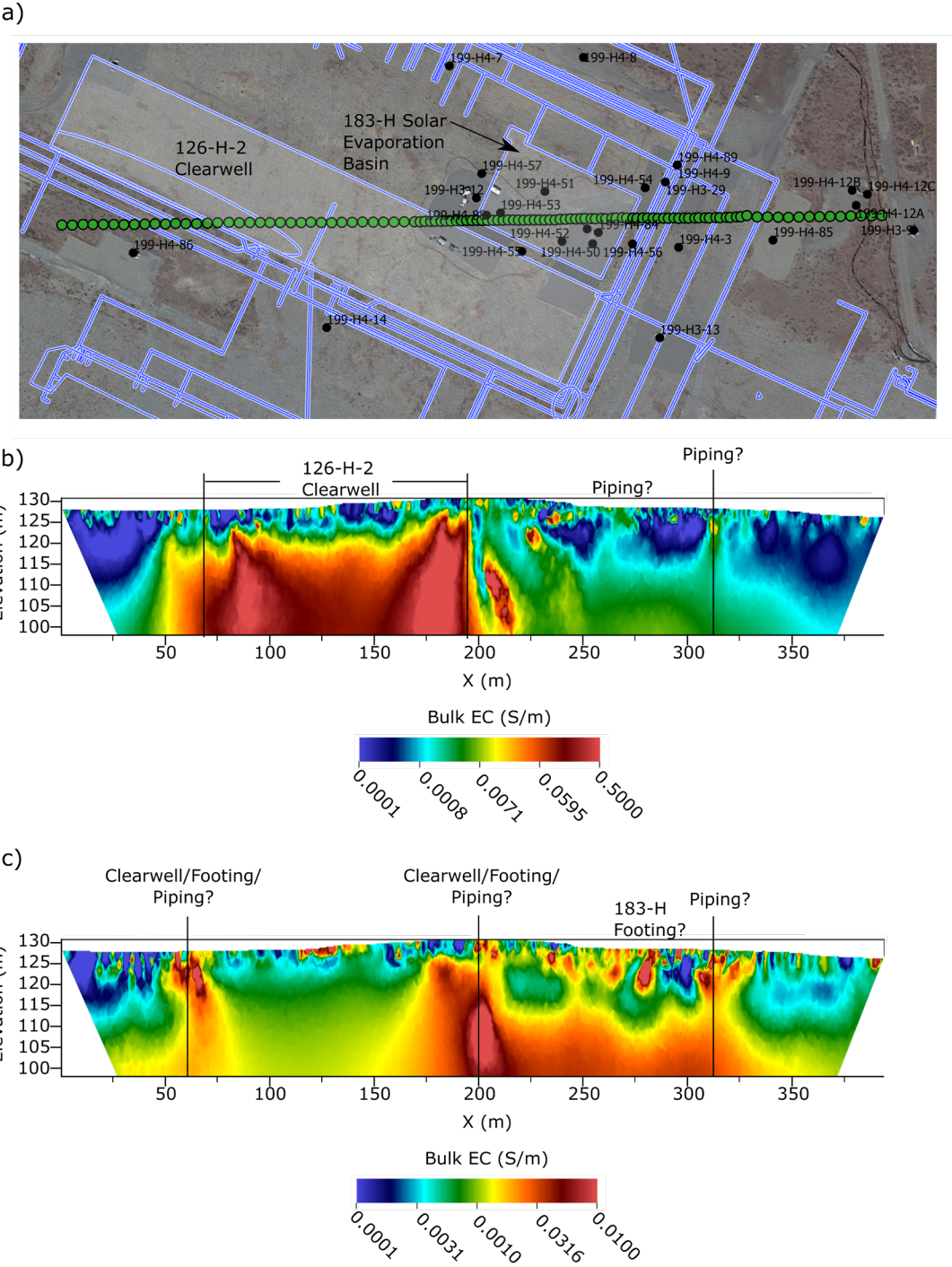
Table 3.1. 100-H ERT line details.

ERT Line Designation	No. Electrodes	Electrode Spacing (m)	Total Length (m)
Line 1	175	2.5 / 5.0	395
Line 1b	64	2.5 / 5.0	192
Line 2	80	2.5 / 5.0	240

The 2D ERT surveys consisted of a combination of larger and smaller dipole offsets to allow for resolution of shallower and deeper features. In addition to filtering measurements for low currents (< 2 mA), high contact resistances (>10 ohm), and poor repeatability (> 5% stacking standard deviations), reciprocal measurements (where current and receiving electrodes are swapped) were collected to assess data quality and provide additional filtering. The E4D constraints included nearest-neighbor smoothing with a preference for a horizontal layered structure. Constraints applied to the E4D modeling are subject to data fit, which means the data must support the model structure shown in the ERT images. Well locations with metallic well casings were incorporated within the E4D modeling.

3.3 Results of 100-H ERT Imaging

The ERT results for line 1 are shown in Figure 3.2. An initial inversion revealed a very large high-conductivity feature that corresponds to the location of the remnants of the former 126-H-2 Clearwell Facility (Figure 3.2b). Historical waste-site decommissioning records suggest that the reinforced concrete floor and wall footings of the Clearwell Facility were left in place. Incorporation of the Clearwell flooring and wall footing features within the E4D modeling resulted in removal of this high-conductivity feature, and is interpreted as a more realistic image in Figure 3.2c. However, imaging electrical structure below this flooring is not possible. Also, there remain several unexplained near-surface and high conductivity artifacts. The E4D algorithm attempts to fit the data to a bulk EC image by increasing the complexity of bulk EC structure. When the data cannot be fit well with a bulk EC image, the complexity increases. For line 1, there is a relatively large occurrence of high-conductivity features and bulk EC surface variability. It is likely there is metallic infrastructure of unknown size, location and shape within this area, which is impacting the fit. This is particularly impactful along line 1, where long dipole offsets interrogate a larger subsurface volume and are more sensitive to the uncertainties affecting current pathways from unknown infrastructure.



The ERT data for lines 1b and 2 were less impacted by metallic infrastructure, and this resulted in ERT images with a better data fit compared to line 1. Lines 1b and 2 show consistency with each other (Figure 3.3a) and show a low EC feature, which decreases in elevation eastward toward the Columbia River shoreline. There is greater variability in the electrical structure to approximately 110 m elevation, but below this there is no differentiation within a high-conductivity region that extends to the bottom of the ERT images. Along line 1b (Figure 3.3b) and line 2 (Figure 3.3c), there are some shallow high-conductivity features, which likely correspond to buried piping or reinforced concrete footings and asphalt pads at the surface.

The top of the high-conductivity feature observed in lines 1b and 2 (Figure 3.3b, c) generally corresponds with the contact between the Hanford formation and the RUM aquitard (Mackley et al., Table 2.1). Figure 3.3c shows the elevation of this hydrogeologic contact for wells 199-H3-22 and 199-H3-13. If this prominent high-conductivity feature is related to the top of the fine-grained RUM aquifer, then the ERT imaging indicates the top of the RUM decreases in elevation toward the Columbia River (eastward). Unknown high-conductivity features (which may be piping) between 199-H3-22 and 199-H3-13 could be limiting the ERT interpretation between these wells; however, this feature does not appear to impact the time-lapse imaging at this location (Section 5.0).

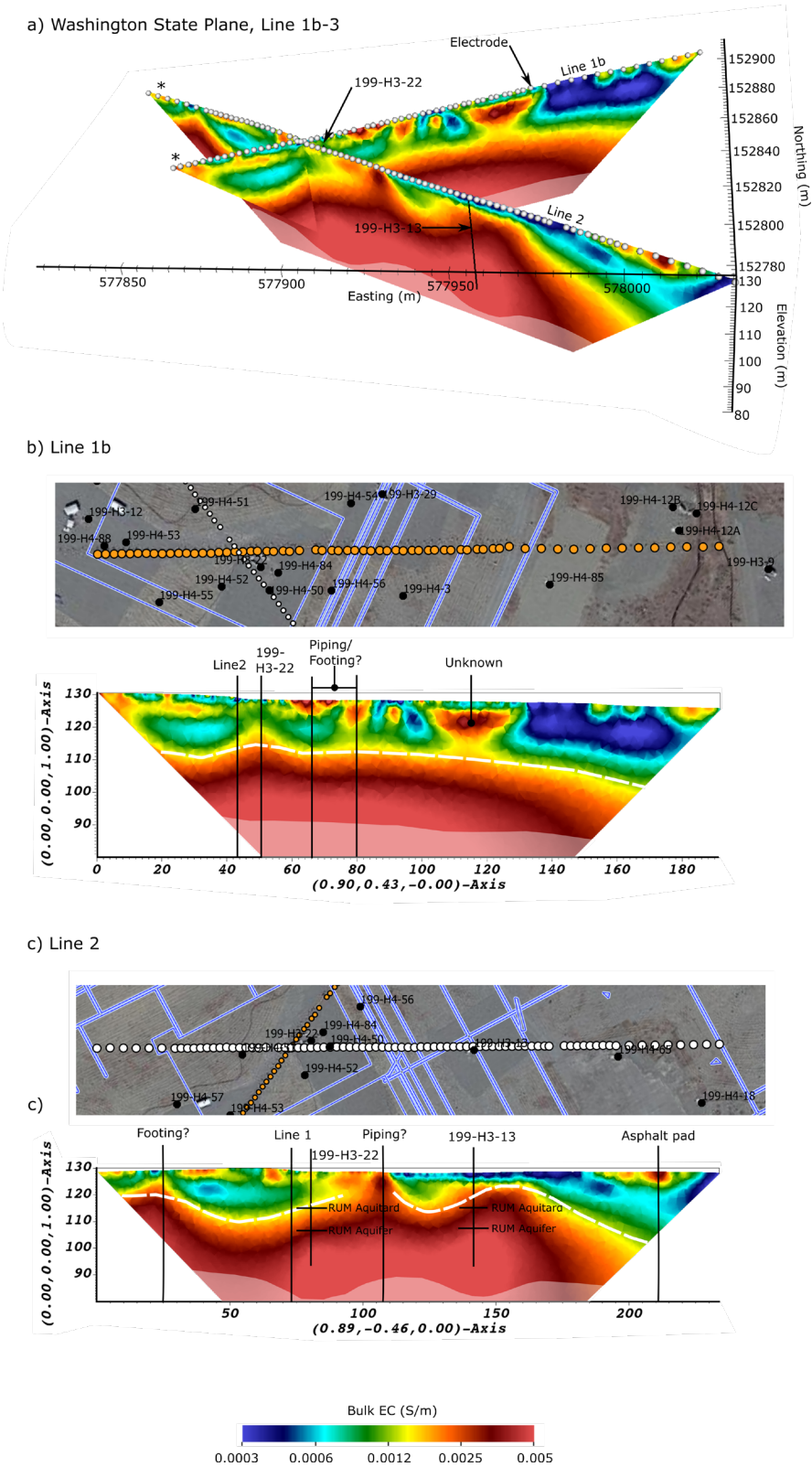


Figure 3.3. ERT images for lines 1b and 2 and Washington State Plane coordinates a) and sectional view of line 1b b) and line 2 c).

4.0 Groundwater F&T Modeling Evaluation

Numerical F&T modeling was performed to (1) provide synthetic but realistic data for evaluating the feasibility of imaging a tracer test in the 100-H Area under different conditions using ERT, and (2) estimate the concentrations of KBr that might reach an extraction well, to evaluate the potential for interference with the IX resin used in the P&T system. The model is only used to support the tracer test evaluation. Bromide tracer concentrations presented in this section and subsequent coupled F&T-ERT simulations (Section 5.0) are reported as mass of KBr per volume of solution to be consistent with input parameters used in the F&T model. In contrast, Br concentrations reported with the laboratory resin evaluations in Section 7.0 are given in terms of mass of the Br ion per volume of solution since laboratory experiments evaluated impacts of the Br⁻ ion on the performance of the SIR-700 ion exchange (IX) resin for treating Cr(VI). Based on the relative atomic masses of K and Br, the Br⁻ concentration is roughly equal to 0.67 times the KBr concentration.

4.1 Model Description

The area of interest surrounds four wells that are part of the HX P&T system (extraction wells 199-H3-22 and 199-H3-29) and well monitoring network (199-H3-12 and 199-H3-13) in the 100-H Area (Figure 4.1). Site characterization data used for model development included (1) elevations of contacts between selected hydrogeologic units at borehole and well locations, (2) hydraulic conductivity estimates from pump test analysis results, and (3) water level data from groundwater monitoring wells (Mackley et al. 2020).

Four hydrogeologic units were considered, which are, from top to bottom, the Hf, the intervening RUM aquitard (also known as the RUM confining layer), the uppermost RUM aquifer (also known as the first water-bearing unit in the RUM), and the underlying RUM aquitard that forms the lower boundary of the uppermost RUM aquifer (Figure 4.1).

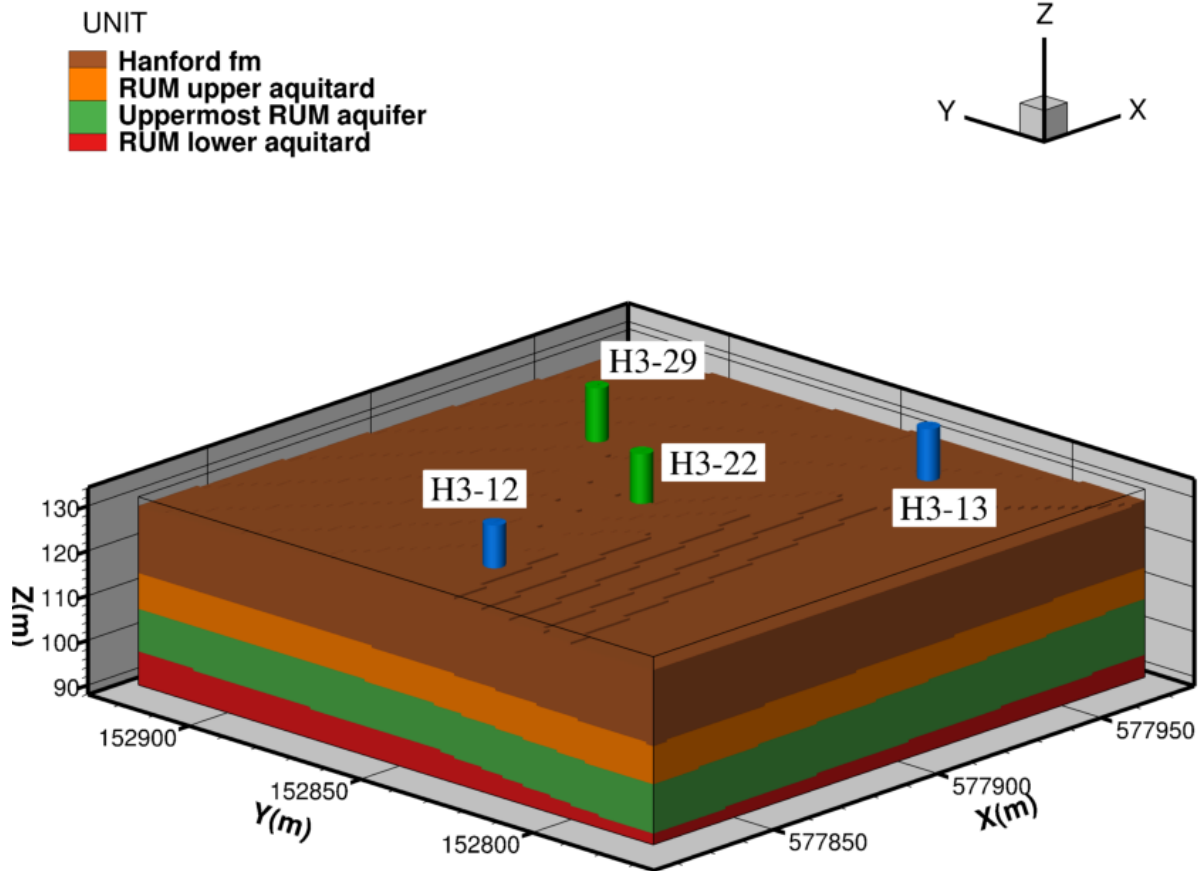


Figure 4.1. Modeled domain showing selected hydrogeologic units at the 100-H Area, with two pump-and-treat extraction wells (199-H3-22 and 199-H3-29) and two monitoring wells (199-H3-12 and 199-H3-13) in the tracer test study area. Note: The standard “199-” prefix on well names in this area is not included in the labels.

A 3D numerical F&T model of the subsurface at the 100-H Area was implemented using the eSTOMP (exascale Subsurface Transport Over Multiple Phases) simulator (Fang et al. 2018). The spatial extent of the model domain was 150 m x 150 m x 42 m in the x-, y-, and z-directions, respectively. Uniform 2-m grid spacing was used in the x- and y-directions, and uniform 0.5-m grid spacing was used in the vertical direction. The top of the model was bounded by the ground surface.

Groundwater flow rates and directions are variable owing to the proximity of the site to the Columbia River and to P&T operations. For the purposes of this study, a constant west-to-east hydraulic head gradient of 2.0×10^{-3} m/m was assumed. The horizontal hydraulic gradient of the RUM aquifer is assumed to be the same as the overlying unconfined aquifer since no published hydraulic gradient information for the RUM aquifer was available. This value represents the average within a range of gradients reported for the unconfined aquifer in the 100-H Area (DOE/RL-2010-95, Rev 0; Table 3-13). This gradient was imposed using constant Dirichlet-type (specified head) boundary conditions on the sides of the model. A constant, Neumann (specified flux) boundary condition of 26 mm/yr was specified for the upper boundary to represent the long-term average natural groundwater recharge rate (Fayer and Walters, 1995; Burbank loamy sand with cheatgrass).

Mackley et al. (2020) recently performed a series of aquifer hydraulic tests in the 100-H Area to quantify transmissivity, hydraulic conductivity, and storage properties of the uppermost RUM aquifer. These tests and associated analyses yielded a range of hydraulic property estimates. Based on these field testing results, a representative value of hydraulic conductivity in the horizontal direction of 5.1 m/day was assumed for the uppermost RUM aquifer. Mackley et al. (2020; Table 5.2) reported a geometric mean value for the vertical hydraulic conductivity of the upper RUM aquitard of 0.013 m/day, so the horizontal hydraulic conductivity of this layer was assumed to be 10 times greater, or 0.13 m/day. The horizontal saturated hydraulic conductivity value for the Hf of 88 m/day was based on SGW-46279 (2016, Table 3.2). Budge (2020; Table 3-1) cites Cole et al. (2001) for estimates of the horizontal hydraulic conductivity of the lower Ringold mud unit ranging from 0.002-0.03 m/day. In lieu of site-specific data for the lower RUM aquitard in the 100-H Area, a horizontal hydraulic conductivity value of 0.008 m/day was used in model simulations for the RUM lower aquitard based on this reported range for the lower Ringold mud. A uniform anisotropy ratio (K_x/K_z) of 10, and a uniform effective porosity of 0.18, were assumed for all units. Parameters that were used in F&T modeling are listed in Table 4.1

Table 4.1. Parameters used in F&T modeling to represent hydrogeologic units (HGU) in the 100-H tracer test study area.

HGU	Saturated hydraulic conductivity in horizontal direction, K_x [m/d]	Anisotropy, K_x/K_z	Porosity
Hanford formation (Hf)	88	10	0.18
RUM upper aquitard	0.13	10	0.18
Uppermost RUM aquifer	5.1	10	0.18
RUM lower aquitard	0.008	10	0.18

4.2 Simulation Results

Simulations were performed for various scenarios involving injection and extraction of different volumes and concentrations of a KBr tracer, for different combinations of the wells shown in Figure 4.1. Two of these wells (199-H3-22 and 199-H3-29) are active extraction wells in the current P&T system. To maintain groundwater extraction in this area during a potential tracer test, modeling efforts focused on scenarios that maintained pumping at typical rates of 30 gpm and 10 gpm for extraction wells 199-H3-22 and 199-H3-29, respectively.

Wells 199-H3-12 and 199-H3-13 were both evaluated as potential injection wells. However, preliminary F&T modeling results, combined with analyses of ERT data (previous and next sections), indicated that ERT imaging of a tracer injected into well 199-H3-12 might not be feasible, owing to interference from buried metallic features. Therefore, subsequent modeling scenarios focused on using well 199-H3-13 as a sole injection well, since the area between wells 199-H3-13 and 199-H3-22 appears to have less interference from buried metallic features and improved ERT image quality.

Effective imaging of a tracer test using ERT may require the use of high concentrations of ionic solutes to create large enough changes in EC for plumes to be imaged. However, using high concentrations of ionic tracers can be problematic for two reasons: (1) high concentrations can result in plume sinking behavior, owing to density effects; and (2) high concentrations of KBr may interfere with the ability of the resin used in the P&T system to remove Cr(VI). Istok and Humphrey (1995) performed two-well tracer tests in a large-scale physical aquifer model containing a homogeneous, isotropic sand pack. They used Br⁻ concentrations ranging from 50 to 1000 mg/L, with corresponding relative densities between 7.5×10^{-5} and 1.5×10^{-3} . Plume sinking was observed at all concentrations. They concluded that density effects should be considered even when using concentrations as low as 50 mg/L.

Seven tracer injection scenarios were evaluated (Table 4.2), representing different injection volumes and tracer concentrations. The first five scenarios were used primarily for predicting peak concentrations at the extraction well. Additional simulations (scenarios 6 and 7), combined with ERT modeling (Section 5.0), were performed to further evaluate the potential use of ERT for monitoring a tracer test. Density effects were accounted for directly in the simulations.

Table 4.2. Modeling scenarios for injection of a KBr tracer into well 199-H3-13.

Scenario	Injection Volume gal (L)	Duration (hr)	Tracer Injection Concentration (mg/L)
1	2500 (9464)	24	100
2	10,000 (37854)	24	100
3	10,000	24	500
4	10,000	24	1000 (1 g/L)
5	10,000	24	10,000 (10 g/L)
6	10,000	24	30,000 (30 g/L)
7	50,000 (189271)	72	100,000 (100 g/L)

Figure 4.2 shows simulated tracer breakthrough curve results for extraction well 199-H3-22 for all seven scenarios listed in Table 4.2. The first six scenarios involve the injection of a KBr tracer into well 199-H3-13, and constant extraction rates of 30 gpm and 10 gpm from wells 199-H3-22 and 199-H3-29, respectively. Owing to its higher extraction rate, and closer proximity to well 199-H3-13, tracer extraction is dominated by well 199-H3-22. Simulated tracer concentrations at well 199-H3-29 are near zero. Consequently, breakthrough curve results for well 199-H3-29 are not shown.

The injection volumes for scenarios 1 and 2 were 2500 gallons (9464 L) and 10,000 gallons (37,854 L), respectively. Peak arrival times are similar, at just over 100 days, owing to the constant extraction rates. However, peak concentrations are different. The predicted peak concentrations are ~0.24 and ~0.92 mg/L for scenarios 1 and 2, respectively, which are >100x less than the injection concentrations.

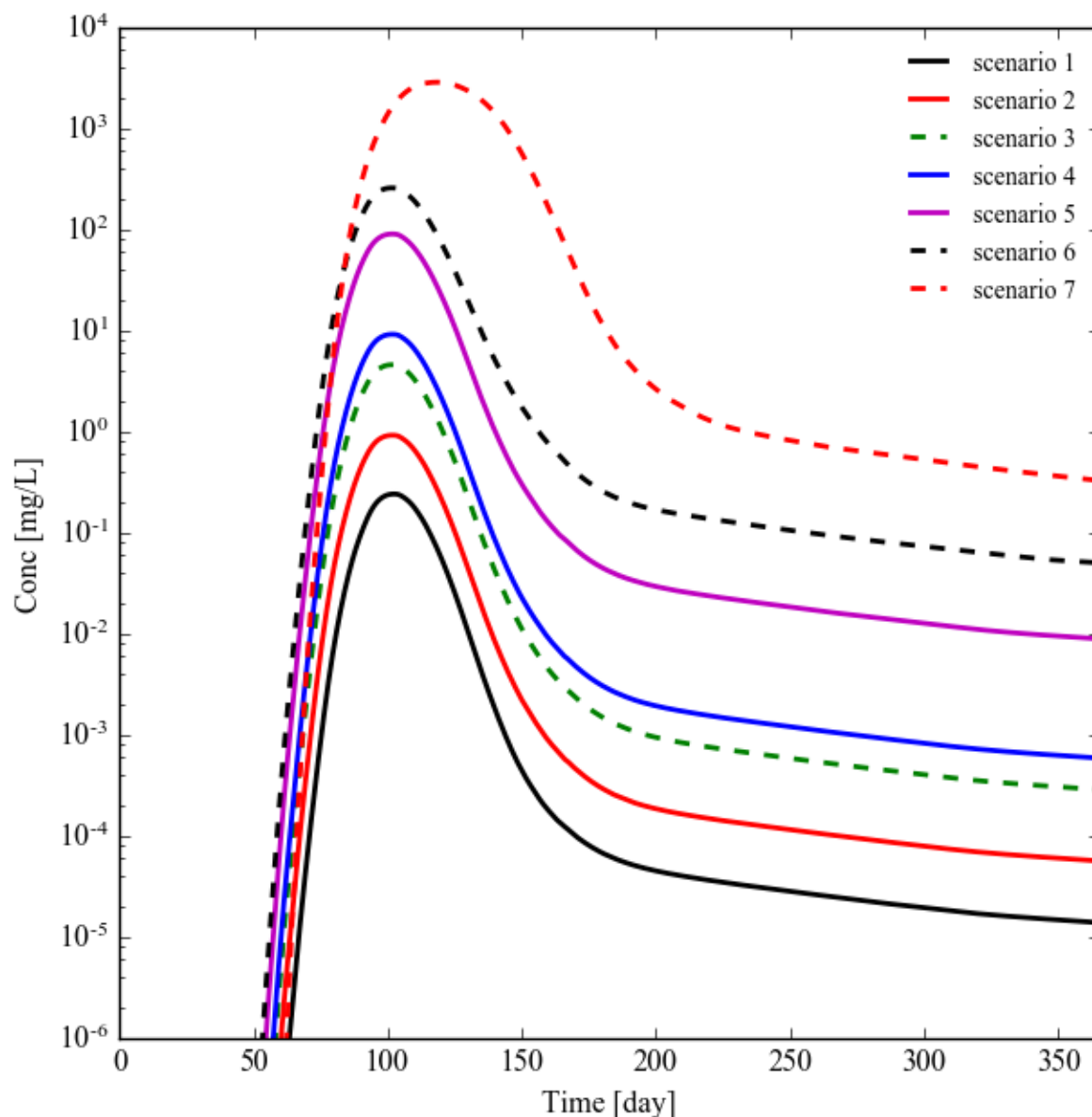


Figure 4.2. Simulated KBr tracer breakthrough curves at extraction well 199-H3-22 for injection concentration and volume scenarios listed in Table 4.1.

The injection concentrations for scenarios 3 and 4 are 500 mg/L and 1000 mg/L, respectively. Peak arrival times for these two scenarios are again similar, at just over 100 days. The predicted peak concentrations are ~4.5 and ~9 mg/L for scenarios 3 and 4, respectively, which again are 100 times less than the injection concentrations.

The injection concentration for scenario 5 was 10 g/L. The peak arrival time is similar to the other cases, again at just over 100 days. The predicted peak concentration is ~90 mg/L, which again is 100 times less than the injection concentration.

The injection concentration for scenario 6 was 30 g/L. The peak arrival time is similar to the other cases, again at just over 100 days. The predicted peak concentration is ~255 mg/L, which is 100 times less than the injection concentration.

The injection concentration for scenario 7 was 100 g/L, the highest concentration used for any of the simulation cases. The peak arrival time is longer than for other cases, at just over 118 days, due to high injection volume for this case. The predicted peak concentration is ~2829 mg/L, which is 30 times less than the injection concentration.

Results from highest-concentration simulation scenarios 6 and 7 (>30 g/L) indicate that fluid density effects result in a small and less concentrated fraction of the injected tracer plume persisting in the lower part of the RUM aquifer at the boundary with the lowermost RUM confining unit for an extended period of time (>1 yr). However, density effects can be reduced if lower injection concentrations are used (e.g., 1 to 10 g/L).

The simulation results for the modeled scenarios are summarized as follows:

- Simulated breakthrough curves in extraction well 199-H3-22 all show peak (max.) concentrations occurring at ~100 days (~3.3 months). Overall, these results suggest that a tracer test could be performed in the RUM aquifer at the 100-H Area within a reasonable time frame (3-6 months).
- Predicted peak concentrations at the extraction well are typically 100 times and 30 times lower than injection concentrations for the 10,000- and 50,000-gallon volume injections, respectively. These results were used in conjunction with results from laboratory-based resin evaluations (Section 7.0).
- Predicted concentrations at the extraction well are more than three orders-of-magnitude lower than the predicted peak concentrations after 1 year, and after 1 year predicted concentrations for all scenarios are < 1 mg/L.

Subsequent sections provide additional information on the evaluation of ERT for monitoring a tracer test, and the effects of a KBr tracer on the IX resin used for extraction of Cr(VI) in the 100-H Area P&T system.

5.0 Coupled F&T Model and Time-Lapse ERT

The numerical F&T model simulations (Section 4.0) were incorporated into additional ERT imaging simulations to provide an improved site-specific representation of the subsurface conditions and a more accurate expectation of the capability and requirements of ERT imaging for monitoring a proposed ionic tracer test.

5.1 Methodology

The workflow of these coupled simulations started with spatially interpolating gridded eSTOMP model output (e.g., saturation and tracer concentration) to an E4D unstructured mesh (Johnson et al. 2017). Next, Archie’s law (Archie 1942) was used as a petrophysical transformation to convert the tracer concentration and saturation to bulk EC. A complete review of this transformation is in Robinson et al. 2020. The changes in bulk EC from the F&T model over time were overlaid on the line 2 ERT image to create the “true” bulk EC images for the tracer study area based on the simulated data. Using the line 2 ERT image allows for the site-specific bulk EC structure to be used as a baseline image, and changes in EC due exclusively to the addition of the ionic tracer can be differenced from the baseline image. From these “true” bulk EC distributions, ERT data was generated during forward modeling to which 2% randomly distributed noise was added to simulate data noise. The time-lapse ERT inversion produces images of bulk EC, which are evaluated against the true bulk EC (Figure 5.1).

The objective of the coupled scenarios was to evaluate the ability of ERT to spatially resolve different tracer volumes and concentrations. These are two controlling factors in that tracer volume impacts the volumetric footprint and tracer concentration impacts the bulk EC contrast. To this end, F&T scenarios 5 and 6 (Table 4.2) with tracer volumes of 10,000 and 50,000 gallons, respectively, were used as end members for evaluation. To vary the tracer concentration, the output concentrations were approximated through a ratio scaling. For example, if an input tracer concentration of 60 g/L was used, to scale the results to 30 g/L, the output concentrations were multiplied by the ratio: $60/30 = 0.5$. Maximum and minimum tracer concentration limits used in the coupled simulations were determined through trial and error; the results shown below represent a range whereby the value of ERT can be assessed.

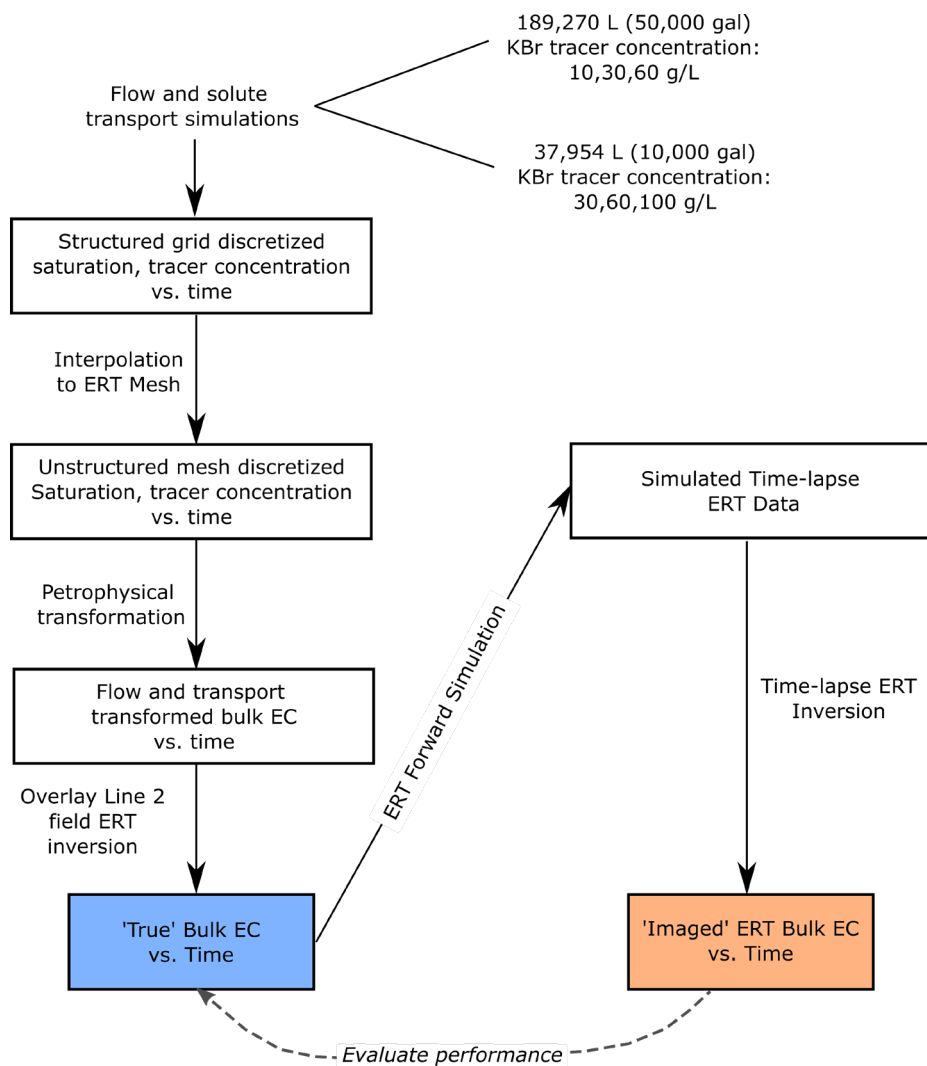


Figure 5.1. Schematic depicting coupled F&T and time-lapse ERT simulations to evaluate ERT feasibility to monitor a tracer injection.

5.2 Results

Results from the evaluation of ERT to spatially resolve different tracer volumes and concentrations are provided below, beginning first with the results for the 50,000 gal scenarios, followed by the results for the 10,000 gallon scenarios. The true (e.g., simulated outputs converted to EC) and ERT imaged (e.g. from E4D) results over time for a tracer volume of 50,000 gallons and tracer concentrations of 10, 30, and 60 g/L are overlain in Figure 5.2. True bulk EC is shown as blue isosurfaces and ERT bulk EC is shown as orange isosurfaces. Time-lapse ERT was able to detect the tracer up until 125 days after the injection and therefore the results are shown up until this elapsed time.

For all tracer concentrations using a 50,000-gallon tracer injection, ERT can spatially identify the location of the tracer between the injection and extraction well as a blurred and/or smeared image of the true location. As the tracer concentration increases, the conductivity contrast increases and the magnitude of the change in the bulk EC increases. For a field experiment, higher concentrations of 30 and 60 g/L would be likely be above site noise levels while 10 g/L may be impacted. ERT resolution is lowest between the injection and extraction wells and this is evident at the 75-day elapsed time (Figure 5.2).

A spatial moment analysis was used to quantify tracer migration behavior shown in Figure 5.2 for the 50,000 gallon simulations. The first moment of the logarithmic changes in bulk EC was used to compute the 2D center of mass for the time-lapse results (Singha and Gorelick 2005). The true and ERT imaged center of mass coordinates are shown in Figure 5.3. At a first glance, the ability of using ERT to precisely identify the center of mass is imperfect, mostly due to limited ERT resolution. However, this result is based on simulated data whereas field-based measurements may provide better resolution than estimated in this assessment.

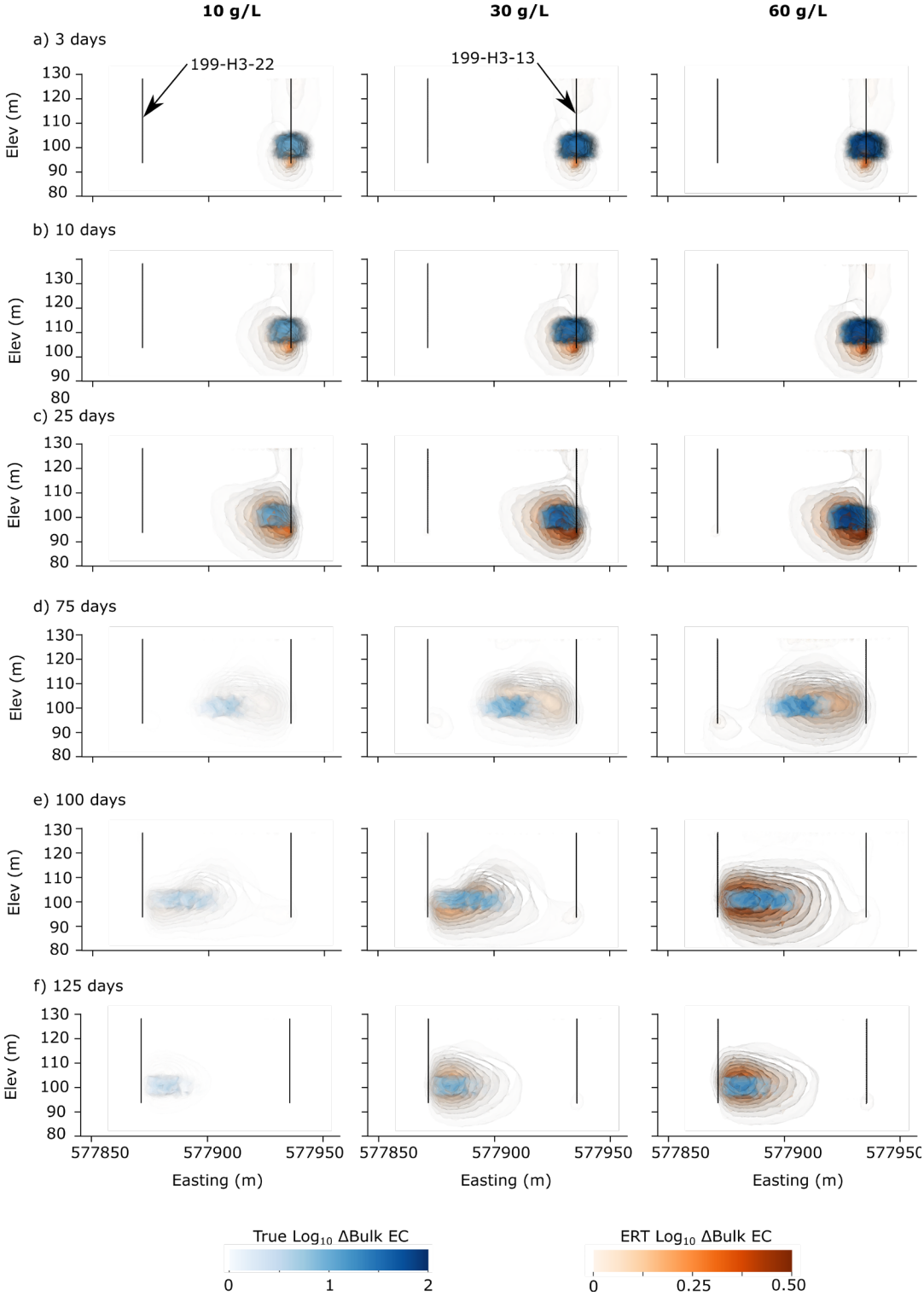


Figure 5.2. Time-lapse images showing true bulk EC from the F&T simulations and ERT bulk EC for a 50,000-gallon tracer injection with a tracer concentration equal to 10, 30, and 60 g/L, where the time elapsed since the tracer injection was a) 3 days, b) 10 days, c) 25 days, d) 75 days, e) 100 days, and f) 125 days.

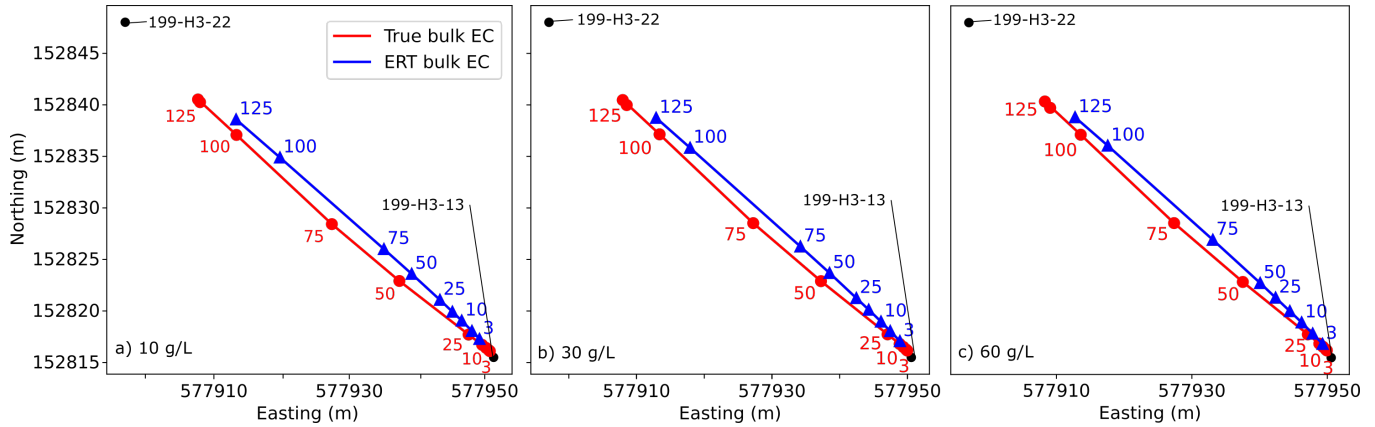


Figure 5.3. Spatial moment analysis comparing center-of-mass estimates for tracer concentrations of a) 10 g/L, b) 30 g/L, and c) 60 g/L at an injection volume of 50,000 gallons.

The results using a 10,000-gallon tracer injection volume at varying tracer concentrations of 30, 60, and 100 g/L are shown in Figure 5.4. Higher tracer concentrations were simulated to provide a sufficient signal for ERT detection relative to the case using 50,000 gallons of tracer. For the lowest concentration of 30 g/L, there was no detection using ERT beyond 25 days. For the higher concentrations of 60 and 100 g/L, ERT can image the tracer until 100 days, after which there is little or no tracer detection. A spatial moment analysis (not shown) for 10,000 gallons demonstrated that ERT was not likely able to effectively monitor the tracer.

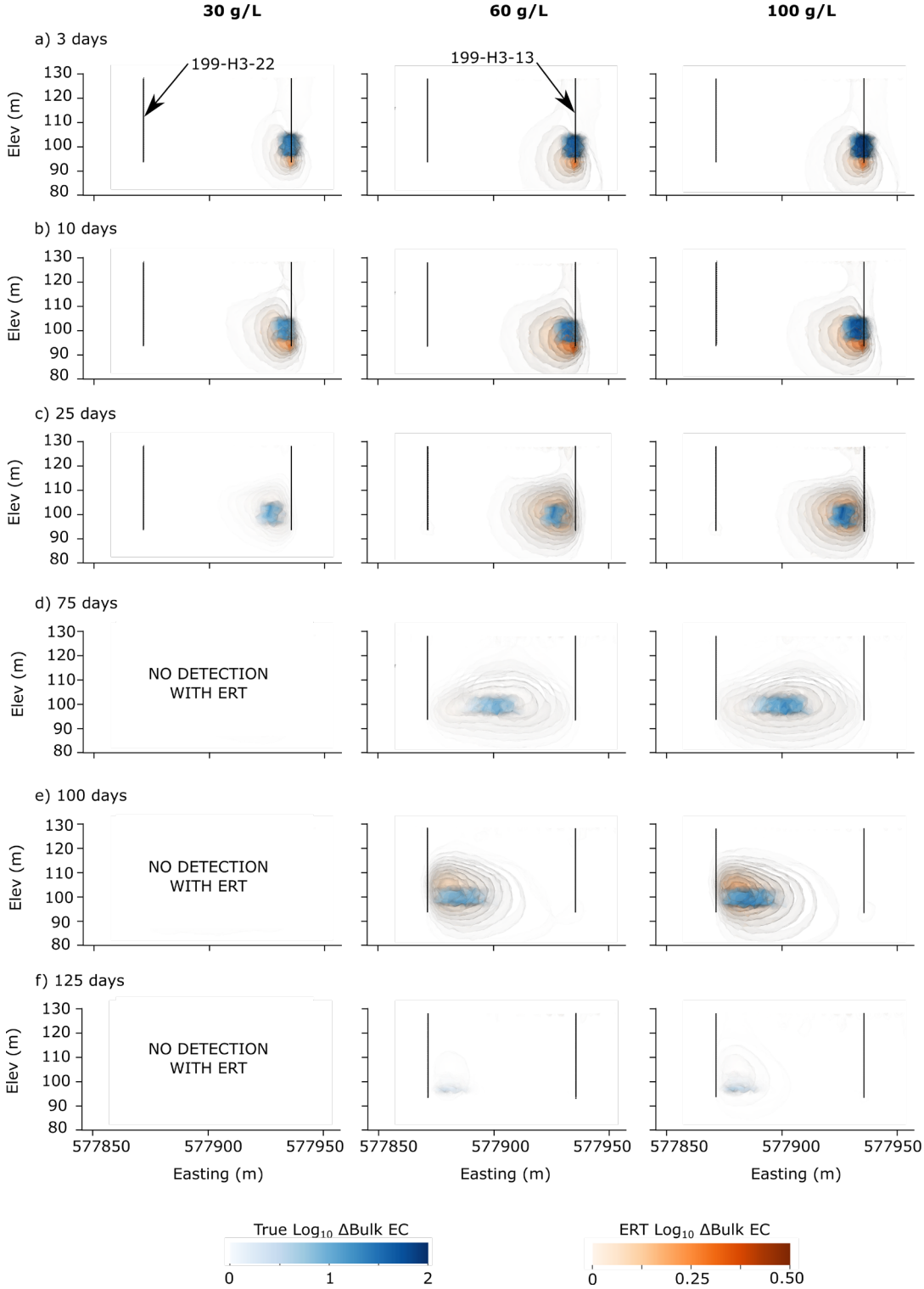


Figure 5.4. Time-lapse images showing true bulk EC from the F&T simulations and ERT bulk EC for a 10,000-gallon tracer injection with a tracer concentration equal to 30, 60, and 100 g/L, where the time elapsed since the tracer injection was a) 3 days, b) 10 days, c) 25 days, d) 75 days, e) 100 days, and f) 125 days.

6.0 Blended Bromide Concentrations in HX P&T System

Results from the coupled ERT-F&T tracer transport simulation (Section 5.0) indicate that monitoring of the Br tracer with ERT would likely require injected KBr tracer concentrations in the range of 10-100 g/L, depending upon the injection volume (Section 5.0). Simulations from the F&T modeling predict about 100:1 and 30:1 for the injected concentration compared to the peak extracted concentration for the 10,000 gallon and 50,000 gallon injection scenarios, respectively (Section 4.0). Based on this, the predicted peak KBr concentrations in extraction well 199-H3-22 are 0.1-1 g/L and 0.3-3 g/L for the 10,000 and 50,000 gallon injection scenarios, respectively (Table 6.1).

Additional blending of the Br tracer solution within the HX influent stream should occur due to the contributions of the other extraction wells according, calculated as:

$$\text{blending ratio } \frac{Q_{HX}}{Q_{EW}} = \sim 15:1 \quad (6.1)$$

$$Q_{HX} = \frac{V_{HX}}{(365 * 24 * 60)} = 1927 \text{ L/min (509 gpm)} \quad (6.2)$$

where:

Q_{HX} = calculated average flow rate of HX P&T system in CY2019

V_{HX} = reported total volume through HX P&T system in CY2019 (1,013 million L [267 million gallons]; DOE/RL-2019-67, Rev. 0)

Q_{EW} = reported average annual flow rate of extraction well 199-H3-22 in CY2019 (124.7 L/min [32.9 gpm]; DOE/RL-2019-67, Rev. 0)

The blending ratio between the extraction and the HX P&T influent calculated using Eqs. (6.1) and (6.2) and pumping rate and volume information for the HX P&T system (DOE/RL-2019-67, Rev. 0) is ~ 15:1. For the range of Br concentrations predicted by the F&T modeling and a blending ratio of ~15:1, the peak Br concentrations in the HX P&T facility are predicted to be 0.007-0.07 g/L and 0.02-0.2 g/L for the 10,000 gallon and 50,000 gallon injection scenarios, respectively (Table 6.1).

Table 6.1. Predicted peak bromide concentrations in extraction well 199-H3-22 and the HX P&T system for a range of tracer concentrations and volumes.

Injection Volume (gal)	Injection Well 199-H3-13	Extraction Well 199-H3-22 ^(a)	HX P&T System ^(b)
10,000	10 to 30 g/L	0.1 to 0.3 g/L	0.007 to 0.02 g/L
50,000	100 g/L	3 g/L	0.2 g/L

(a) Based on F&T modeling results (Section 4.0).

(b) Based on blending ratio of ~15:1 calculated with Eqs. (6.1) and (6.2) using pumping rate and volume information from DOE/RL-2019-67, Rev 0.

7.0 Laboratory Evaluations of Bromide and SIR-700 Resin

Laboratory experiments were performed to directly evaluate potential impacts of a Br tracer on the SIR-700 IX resin used in the HX P&T system for Cr(VI) treatment. Results from the coupled ERT-F&T tracer transport evaluations (Section 5.0) suggest monitoring of the Br tracer in the RUM aquifer with ERT might require injected concentrations between of 10 and 100 g/L, depending upon the injection volume (Section 5.0). Even with the significant decrease in the extracted and blended concentrations of Br (Table 6.1), the potential for Br to negatively impact the performance of the SIR-700 ion at the highest injection concentration and volume scenarios could be a concern. The objectives, methodology, and results of laboratory experiments evaluating Br impact to resin performance are described in this section.

The two primary objectives of the laboratory experiments were to:

1. Identify the potential impacts of a Br-bearing anionic tracer, such as KBr, at varying Br and Cr(VI) concentrations on the performance of the ResinTech® SIR-700 IX resin used in the HX P&T system for treating Cr(VI) in groundwater (DOE/RL-2019-67, Rev. 0).
2. Identify possible interferences from Br associated with a potential tracer test and other anions at similar concentrations to the ones measured in the influent/effluent of the HX P&T system.

A series of batch and column laboratory experiments were designed to address these objectives over a range of Br and Cr(VI) concentrations. The batch experiments were performed first since they are a less expensive method for evaluating many different combinations of Br and Cr concentrations. Column tests were used to simulate the flow and Cr treatment conditions of the SIR-700 resin in the HX P&T facility. The results from the batch tests were used to determine the influent concentrations of Br and Cr for the column experiments.

Tracer concentrations reported for the laboratory experiments are given in terms of mass of the bromide ion (Br⁻) per volume of solution due to this section's focus on ionic impacts of the Br tracer solution on the performance of the SIR-700 IX resin for treating Cr(VI). In contrast, tracer concentrations reported during other portions of the evaluation (e.g., F&T modeling, coupled F&T-ERT simulations, and predicted Br concentrations) are reported as mass of KBr per volume of solution to be consistent with input parameters used in the F&T model. Based on the relative atomic masses of K and Br, the concentration of Br⁻ in the tracer is equal to 0.67 times the KBr concentration.

7.1 Batch Tests

The methods and results of the batch testing are detailed in Appendix A. In summary, results from the batch tests found Br removal occurs at all tested Br concentrations, although the percent removal decreased with increasing Br concentration. The amount of Cr removed was also found to diminish at high Br concentrations (30,000 mg/L). These results suggest that (in a static system) concentrations of Br at 30,000 mg/L impede removal of Cr by the SIR-700 resin, but this inhibition is minimal when Br concentrations are at or below 1000 mg/L. The mechanism of Br retention in the batch tests may result in an accumulation of Br that causes an inhibition of Cr removal, even at lower influent Br concentrations. However, the batch test results were valuable for informing the design for the column experiments that better represent the flow-through conditions in the HX P&T system.

7.2 Column Tests

The batch experiments were used for screening and design of the column experiments that represent the continuous influx of Br and Cr anticipated at the HX P&T system.

7.2.1 Methodology

Three 1D flow column experiments were conducted to evaluate potential impacts on Cr removal under simulated Br tracer test conditions. The SIR-700 resin was exposed to elevated influent Br concentrations, and outflow from the column was monitored until conditions returned to pre-tracer test values. The experiments were conducted using polyvinyl-chloride (PVC) columns that were 60 mm long, with an inside diameter of 24 mm, and with porous frits at each end. The following is a brief description of the experimental matrix:

1. Three 1D flow columns were packed with resin obtained from ResinTech®. Columns were packed with resin pre-saturated with Br- and Cr-free groundwater to ensure optimal packing density. The resin expands when wet, so pre-saturating the resin ensured sufficient pore space to enable flow after the experiment started.
2. A target Cr concentration of about 300 µg/L was used in all three columns experiments (Table 7.1).
3. Columns 1 and 2 tested the effects of Br concentrations at 1000 and 30,000 mg/L, respectively (Table 7.1).
4. Column 3 tested the effects of Br concentrations at 100 mg/L (Table 7.1). The concentrations of anions, such as Cl, NO₃, and SO₄, were also increased to better match influent/effluent concentrations in the HX P&T facility.
5. The flow rate through the columns was adjusted to achieve a fluid residence time of 15 minutes with the SIR-700 resin, similar to the HX P&T system.¹

Table 7.1. Bromide and chromate concentrations used in column tests.

Column Number	Br Concentration (mg/L)	Cr Concentration (µg/L)
1	1000	300
2	30000	300
3	100	300

The resin was pre-treated prior to use to remove any residual metals or anions left over from the manufacturing process. This was accomplished by placing the resin on a shaker for 1 hour with double deionized (DDI) water at a solution-to-solid ratio of 3:1, followed by centrifugation at 1700 rpm for 5 minutes. After decanting the second wash water, the resin was put in container with DDI water for 24 hours. The excess water was removed after a day and the resin was stored at room temperature until the start of the tests. The columns were packed with resin pre-saturated with Br- and Cr-free simulated groundwater (SGW).

¹ Personal communication from Dean Neshem (Central Plateau Cleanup Company) to Rob Mackley (Pacific Northwest National Laboratory), 09/20/2021.

Br and Cr influent spiked solutions were prepared by adding the appropriate amount of potassium Br and sodium chromate to the same SGW formulation used in the batch tests (Appendix A, Table A.1). Continuous flow column experiments were conducted with the first two columns (with Br concentrations of 1000 and 30,000 mg/L, and target Cr concentrations of about 300 µg/L) to quantify Cr uptake by SIR 700 and the effect of Br concentration on resin performance.

A third column experiment was conducted (the column was packed with the resin in a similar way as the previous two columns). This column was run initially for about 200 pore volumes with a Br-free SGW solution (Appendix A, Table A.1) with a target Cr concentration of about 300 µg/L. The SGW formulation used for the third column included increased concentrations of the major anions, sulfate, nitrate, and chloride to target concentrations of 80, 20, and 10 mg/L, respectively, to better simulate observed concentrations in HX P&T influent. The column was then leached with the same SGW spiked with 100 mg/L Br for about 500 pore volumes, followed by the initial Br-free solution for an additional 500 pore volumes. The column was then spiked a second time with 100 mg/L Br for ~300 pore volumes before switching back to the initial Br-free solution. The Br-free solutions were run continuously until effluent concentrations were below the limit of quantification; this was done to evaluate the potential for contaminant release from the resin and quantify the mass of Br retained.

For column 3, stop-flow events were applied to determine time-dependent rates of removal for both Cr and Br and pH changes during and after the stop-flow events. For all three columns, select influent and effluent samples were collected and analyzed for total Cr and Br. The pH was measured for each of the samples immediately after collection. Changes in pH are important because the SIR-700 resin is designed for optimum Cr removal at a pH of ~6. Batch test results identified high concentrations of Br in solutions with an elevated pH. The pH of the influent solution of the column experiments was initially adjusted to ~5. In all columns, the pH of the effluent solution was higher than the pH of the influent solution, with no significant changes in pH (6.7 to 7.6).

Effluent samples were collected with a fraction collector in vials; an average tare of 10 vials was used as an average tare for all vials. The vials were weighed after collecting effluent to determine the quantity of solution that passed through the column. This mass was used to calculate the flow rate through the columns throughout the experiments.

7.2.2 Br Results

In column 1, the breakthrough was observed after ~6 pore volumes (Figure 7.1). In column 2, the breakthrough was observed between ~19 and ~110 pore volumes (the actual breakthrough was not captured; Figure 7.2). In column 3, the Br breakthrough was observed after ~40 pore volumes (Figure 7.3). Following the breakthrough, the effluent Br concentration of columns 1 and 2 approximately matched the influent concentration for the remainder of the experiment. Effluent Br concentrations in column 3 continued to increase past influent concentrations after the breakthrough curve, reaching a maximum concentration of ~124 mg/L (24% higher than the influent concentration), indicating desorption of the previously adsorbed Br. The effluent concentration then decreased to approximate influent concentrations. This trend was repeated in column 3 during the second Br spike – the concentration increased to ~104 mg/L (4% higher than the influent concentration) and decreased to approximate the influent concentration once the influent solution was absent of Br.

The mass of Br retained by each column was quantified by calculating the difference in area between the influent and effluent Br breakthrough curves. Br resin retention was consistent for columns 1 and 2. By the end of the experiment, column 1 had retained 2666 mg of Br (0.38 g per gram of dry resin) and column 2 had retained 2415 mg of Br (0.37 g per gram of dry resin).

Retention and remobilization results for column 3 varied during the multiple Br spiking and release events included in the experiment. During the first Br spike, column 3 retained ~125 mg of Br (~17 mg per gram of dry resin). This mass of Br reached a maximum after 331 pore volumes, decreasing to ~97 mg (~13 mg per gram of dry resin) after reaching equilibrium. After the column 3 influent was switched to a Br-free solution, approximately all of the Br was remobilized within <200 pore volumes. During the second Br spike, column 3 retained ~184 mg of Br (~25 mg per gram of dry resin). After this spike in Br retention, the amount retained decreased to ~98 mg (~13 mg per gram of dry resin) after reaching equilibrium. After the column 3 influent was changed to the Br-free solution a second time, ~41 mg of Br was retained in the column (~5 mg per gram of dry resin) after reaching equilibrium.

The decreased Br retention in column 3 relative to columns 1 and 2 is likely due to competing interactions between Br and other anions (particularly sulfate; Figure 7.4). The sulfate breakthrough occurs ~100 pore volumes after the Br breakthrough, suggesting a preferential adsorption of sulfate over Br (Figure 7.4). Additionally, when the influent solution was changed to the Br-free solution, the effluent sulfate concentration dropped significantly, suggesting the sulfate is quickly retained by the resin as soon as the Br is desorbed. Alternatively, the relatively lower Br retention exhibited in column 3 could be explained by a concentration-dependent adsorption of Br by the SIR-700 resin, where lower Br concentrations result in lower retention rates.

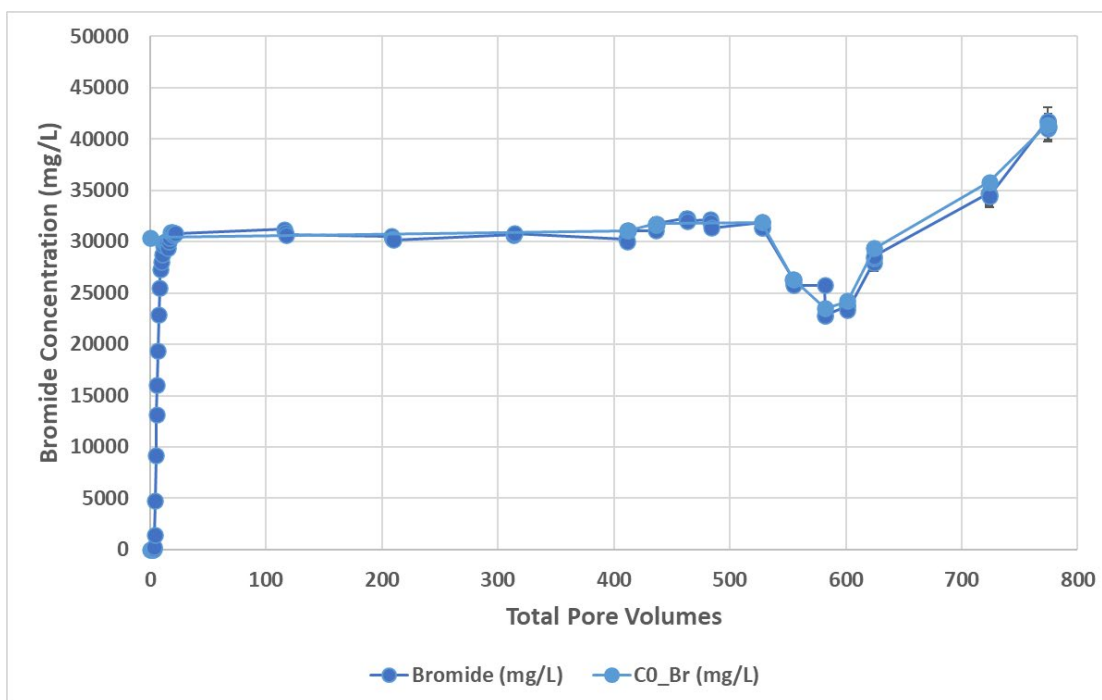


Figure 7.1. Column 1 influent Br concentration (light blue) and effluent Br concentration (dark blue) versus number of pore volumes.

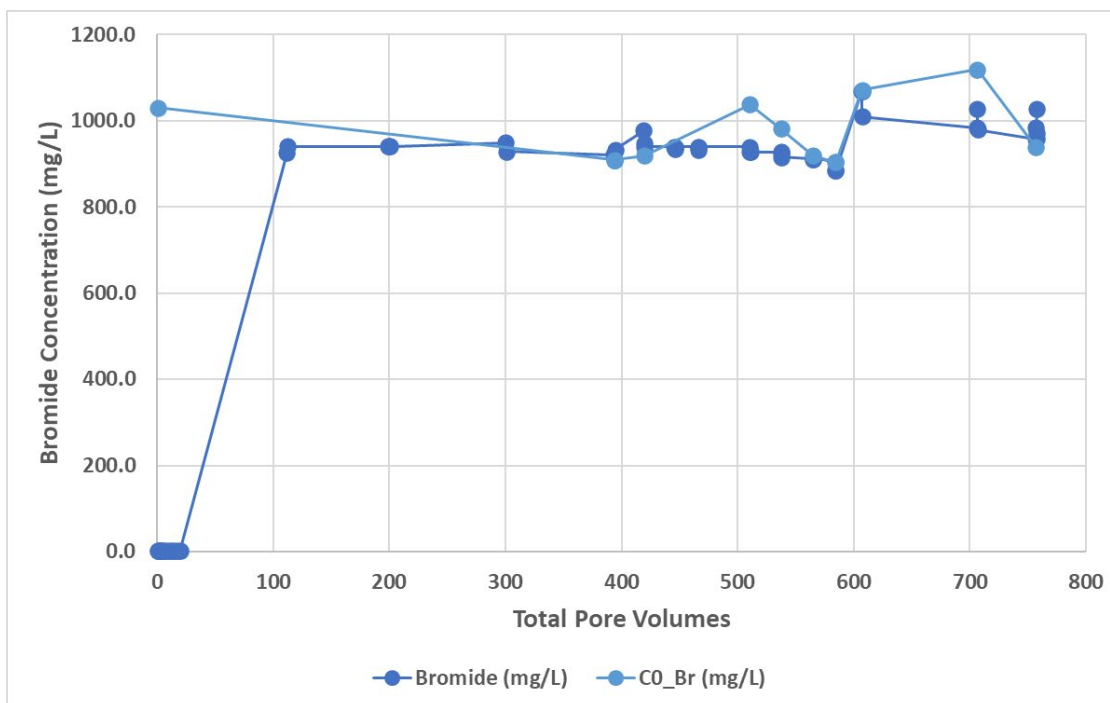


Figure 7.2. Column 2 influent Br concentration (light blue) and effluent Br concentration (dark blue) versus number of pore volumes.

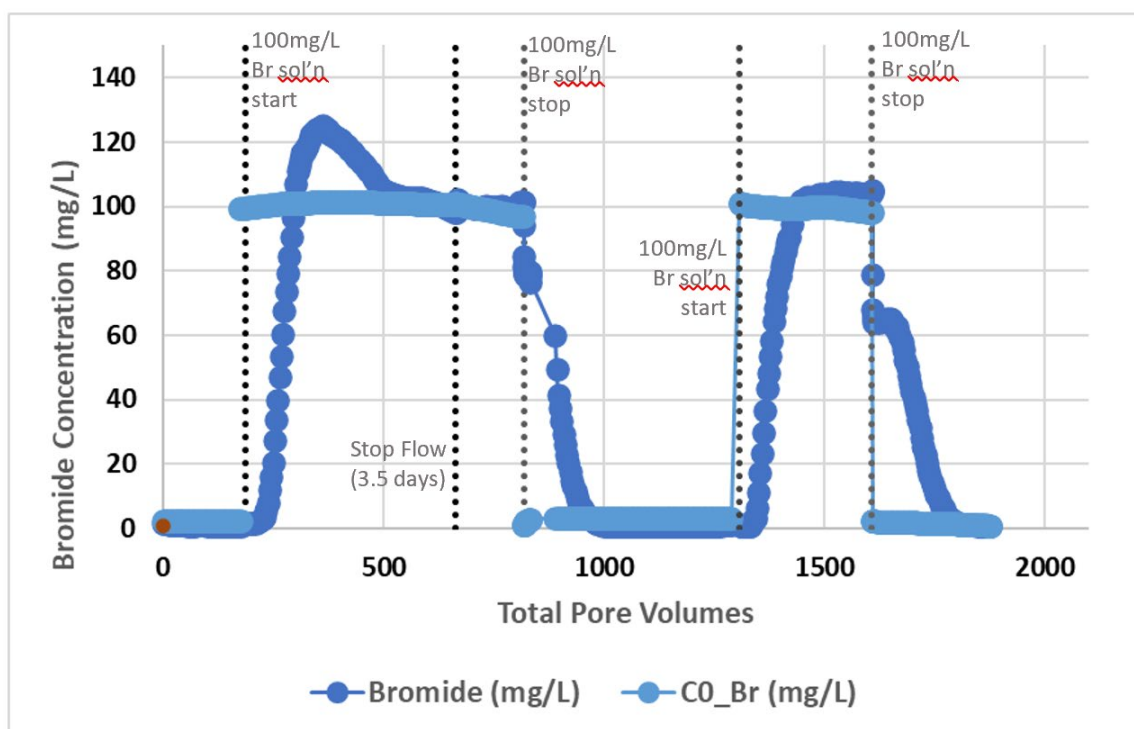


Figure 7.3. Column 3 influent Br concentration (light blue) and effluent Br concentration (dark blue) versus number of pore volumes.

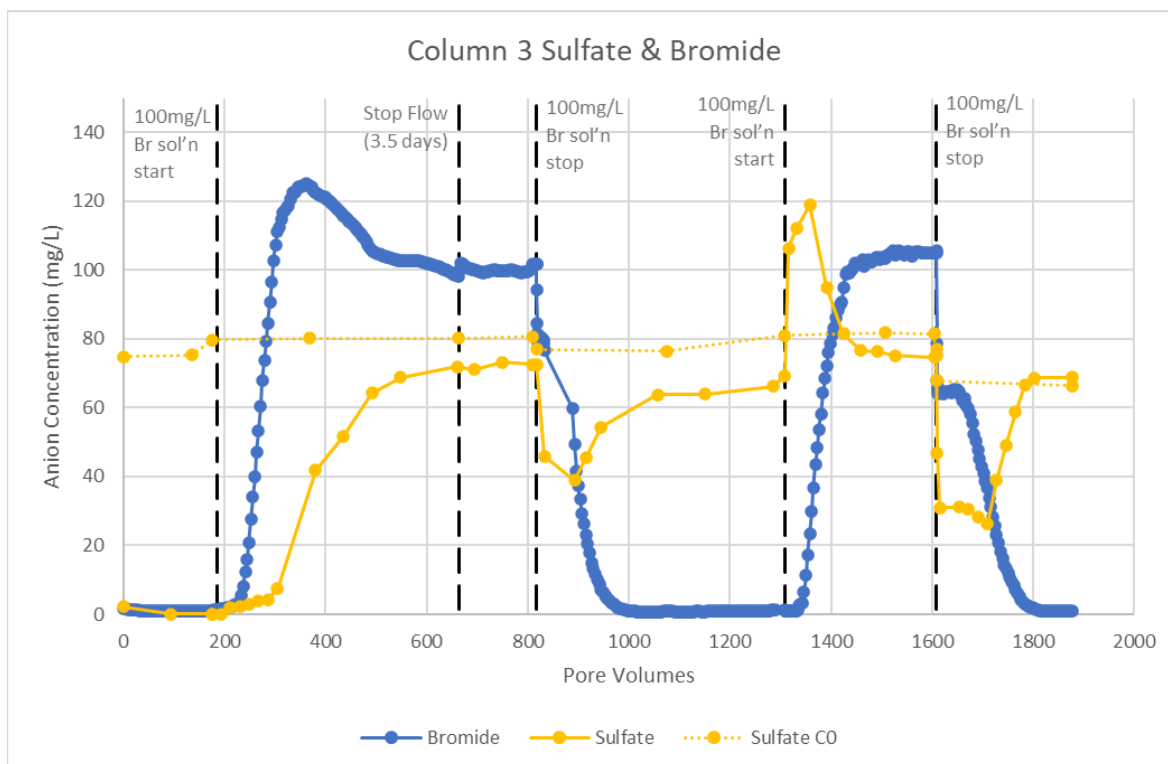


Figure 7.4. Concentrations of column 3 influent sulfate (yellow dotted line), effluent sulfate (yellow solid line), and effluent bromide (blue) versus number of pore volumes. Target influent Br concentration was 100 mg/L. Note: sulfate concentrations >100 mg/L and <5 mg/L were outside the calibration range.

Aqueous Br was most likely removed by the SIR-700 resin via an anion exchange reaction, but the reaction is reversible. Nearly all of the adsorbed Br was released in the aqueous phase when the resin was leached with a Br-free solution. In the HX P&T system, the Br tracer would likely be temporarily retained until the concentration-dependent retention capacity for Br is reached. At that point, the effluent Br concentration would increase to match influent concentrations. As influent concentrations decrease, any retained Br would be released over time.

7.2.3 Cr Results

In column 1 (300 µg/L Cr and 30,000 mg/L Br), chromate concentrations remained low throughout the first 15 pore volumes before increasing to ~60% of the influent concentration (Figure 7.5). Chromate removal remained approximately constant throughout the experiment, with an average of ~112.18 µg/L removed per liter of influent solution (about 38% removal). In column 2 (300 µg/L Cr and 1000 mg/L Br), approximately 99.6% of chromate was removed (Figure 7.6). In column 3 (300 µg/L Cr and 100 mg/L Br), Cr concentrations in the influent remained around 300 µg/L for the duration of the experiment while effluent concentrations remained near or below detection for most of the experiment, except for spikes at ~186, ~1308, and ~1608 pore volumes (Figure 7.7). The spikes lasted for a short period of time and possibly indicate complex interactions among anions present in the influent solution, suggested by the decrease in effluent sulfate concentrations that occurred during these spikes. The spikes in Cr in the effluent may be caused by temporary fouling of the SIR-700 resin due to the high concentration of Br in the influent solution. Also, preferential adsorption of Br to the surface of the resin may be causing Cr to desorb and exit the column.

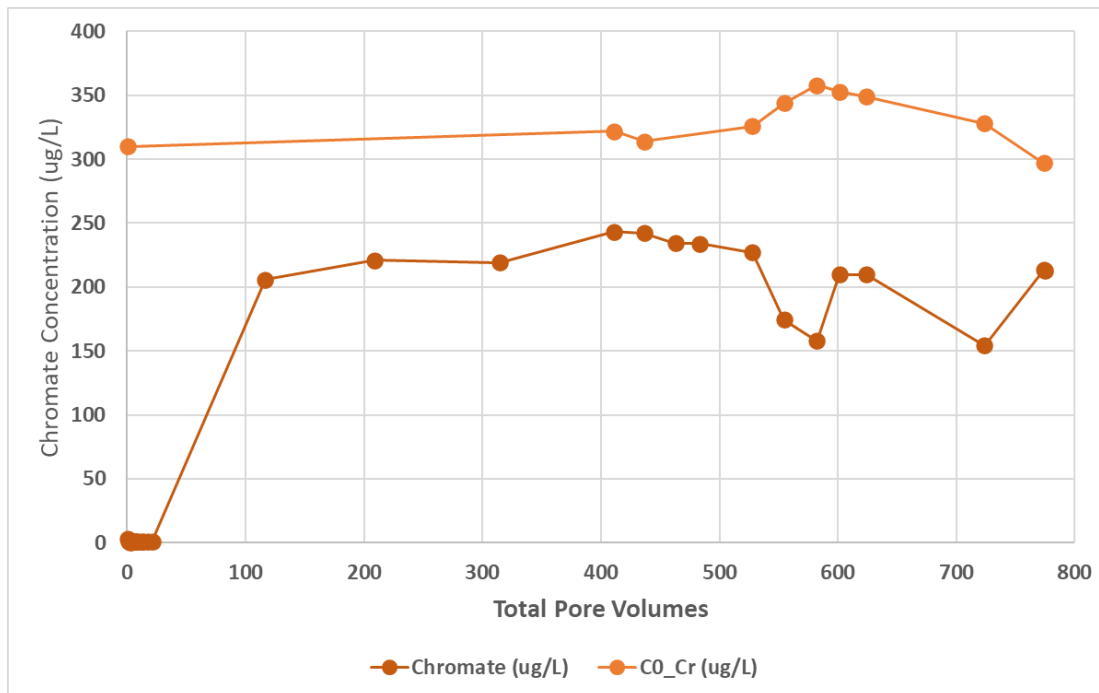


Figure 7.5. Column 1 influent chromate concentration (light orange) and effluent chromate (dark orange) versus number of pore volumes. The targeted influent Br concentration for this column was 30,000 mg/L.

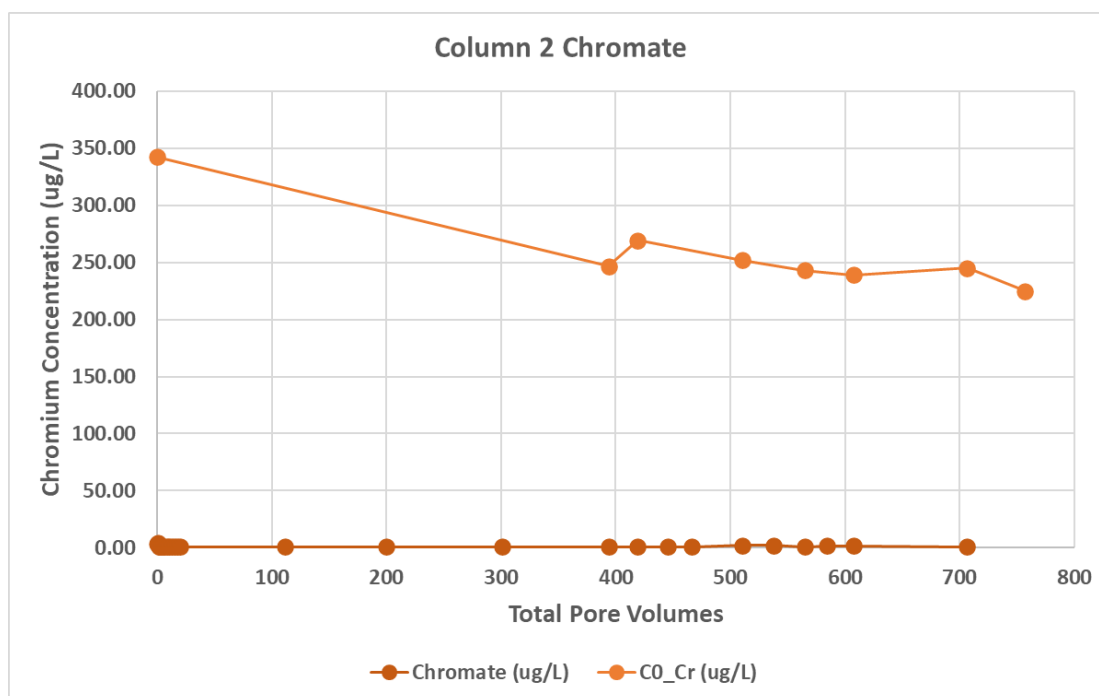


Figure 7.6. Column 2 influent chromate concentration (light orange) and effluent chromate (red) versus number of pore volumes. The targeted influent Br concentration for this column was 1000 mg/L.

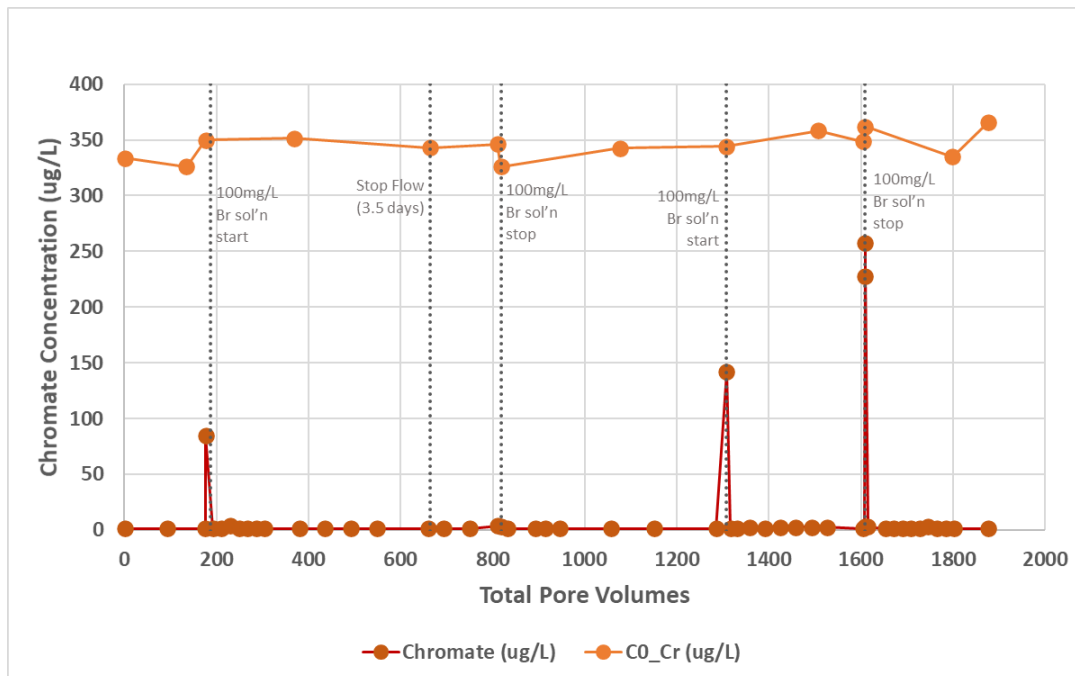


Figure 7.7. Column 3 influent chromate (orange) and effluent chromate (dark orange) versus number of pore volumes. The targeted influent Br concentration for this column was 100 mg/L.

Similar to the batch experiments, column tests indicate Br concentrations <1000 mg/L do not impact removal of Cr by the SIR-700 resin. However, a significant impact to resin performance can occur for Br concentrations of 30,000 mg/L or greater. For tracer testing, this suggests that regardless of the total tracer mass, as long as the Br concentration reaching the HX P&T system is ≤ 1000 mg/L, the Cr removal efficiency should be minimally influenced. When designing a potential tracer test, the concentrations of Br reaching the HX P&T system should be considered in relation to the performance of the SIR-700 resin.

8.0 Integrated Evaluation Discussion and Conclusions

The results from the field ERT investigations, numerical F&T modeling, coupled ERT-F&T model simulations, and the laboratory resin experiments presented in the previous sections provide the technical basis for evaluating a variety of tracer test scenarios in the RUM aquifer within the 100-H study area. This section presents an integrated discussion of the evaluation results with respect to the key evaluation considerations discussed in Section 2.4. These include:

- RUM aquifer hydrologic characterization as identified in the RD/RA WP (DOE/RL-2017-13, Rev. 0)
- Minimal impact to operations or remedial performance
- Utilization, if possible, of time-lapse ERT for monitoring tracer transport

The numerical F&T modeling and laboratory experiments used in this evaluation were designed to represent, to the extent possible, the site-specific hydrogeologic, tracer test configuration, and groundwater flow and tracer transport conditions at the field scale and within the HX P&T facility. However, there are inherent limitations and uncertainties associated with forward modeling and lab-to-field upscaling. The results can and should be used as the technical basis for a go/no-go decision for implementation and final test design. However, the results should not be overinterpreted or considered exact predictions of what may occur in a highly heterogeneous hydrogeologic setting.

8.1 Outcome and Remedial Impact

The F&T modeling simulations indicate that forced-gradient (convergent flow) tracer tests will provide quantitative data that can be used to estimate aquifer hydraulic and transport properties for the uppermost RUM aquifer. For Br tracer test scenarios with injection volumes and concentrations of at least 10,000 gallons and 10,000 mg/L, respectively, the expected peak tracer concentration in the extraction well (199-H3-22) is about 100 mg/L (Table 6.1). The range of Br concentrations on the breakthrough curves at these peak concentrations can be readily distinguished from background (<1 mg/L; DOE/RL-96-61, Rev. 0) and are well above typical detection limits using ion chromatography methods (<0.5 mg/L). Breakthrough curves are expected to have sufficient resolution to be quantitatively analyzed with F&T numerical modeling or analytical solution methods to estimate aquifer hydraulic and tracer transport properties such as effective porosity, groundwater velocity, and longitudinal dispersivity. These are critical input and calibration parameters needed for predictive analyses that support decision-making for remedies associated with the RUM aquifer, such as the optimum number and location of P&T wells.

8.2 Compatibility with HX P&T System

From the onset of this evaluation, it was recognized that shutting down multiple P&T extraction wells in the RUM aquifer for extended time periods to accommodate a tracer test would negatively impact Cr(VI) removal and likely would be viewed as unacceptable. As discussed below, the numerical F&T modeling (Section 4.0) and laboratory resin experiments (Section 7.0) support the conclusion that tracer testing can be compatible with the P&T system and still provide the hydrologic characterization information needed for the RUM aquifer.

8.2.1 Operational Impacts

The use of wells 199-H3-13 and 199-H3-22 as injection and extraction wells, respectively, in a forced-gradient tracer test configuration will not require any major changes to P&T operations in terms of continuity of pumping. Since no P&T wells will need to be shut down for more than a day at the beginning and end of the tests to support installation of instrumentation, there will be little to no impact on the overall volumetric and mass removal performance of the HX P&T system. F&T modeling indicates it will take 3 to 4 months for peak arrival of the tracer and a total duration of about 6 months to capture the entire breakthrough curve (including the return to near-zero Br concentrations).

The footprint of the 100-H tracer test study area (Figure 2.3) is large enough to accommodate tracer injection equipment (portable purge tank, field lab and injection control process trailers, portable generator, etc.). The injection design will need to be finalized in field procedure and test instruction documents; however, it is expected that the tracer injection portion of the test will last only a few days. Tracer injection and ERT monitoring are not expected to be impact local access to roads in the study area.

8.2.2 SIR-700 Resin Performance Impacts

Potential performance impact to the SIR-700 IX resin by the Br tracer was a significant component of the evaluation. The results from the laboratory column experiments indicate no impact to Cr(VI) removal when the resin is exposed to Br concentrations of 1000 mg/L or less (Figure 7.6 and Figure 7.7). Even for the maximum Br tracer injection volume (50,000 gallons) and concentration (100 g/L) scenario considered in this evaluation (i.e., designed to increase signal for ERT imaging), the predicted concentration of Br running through the SIR-700 resin within the HX P&T system would be ~200 mg/L due to the combined effects of dilution in the extraction well and blending by influent from other P&T extraction wells (Table 6.1). At a lower injection volume and concentration of 10,000 gallons and 10 g/L, the predicted blended Br concentration in the HX P&T system is <10 mg/L (Table 6.1). The laboratory experiments support the conclusion that a Br tracer test can be designed to avoid impacts to the SIR-700 resin for this configuration of injection and extraction wells and range of injection volumes and concentrations.

8.2.3 Effluent Bromide Concentrations

Laboratory flow column experiments consistently demonstrated the SIR-700 resin has a limited retention capacity for aqueous Br (Figure 7.1 through Figure 7.4). The resin's exact retention capacity for Br is concentration-dependent and affected by the presence of other anions (particularly sulfate) (Figure 7.4). Although the initial Br tracer breakthrough appears to be delayed due to adsorption by the resin, the effluent Br concentrations match the influent within 82 pore volumes (equivalent to <1 day under typical HX P&T flow rates). This has important implications for the design of a potential tracer test in terms of effluent concentrations and potential regulatory or environmental limits for Br concentrations being injected into aquifer via P&T injection wells. Blended influent Br concentrations are not expected to decrease within the P&T facility at the timescales and flow volumes relevant to field tracer tests.

Release of retained Br from the resin will occur as Br concentrations decrease following the peak breakthrough portion of the tracer test. Column flow tests indicate nearly all of the adsorbed Br is released from in the aqueous phase when the resin was leached with a Br-free solution. The release rate of Br from the SIR-700 resin is relatively slow and does not result in a high-concentration pulse of Br (Figure 7.3). Effluent Br concentrations would be expected to decrease more slowly in the HX P&T system following peak tracer arrival compared to the flow column experiments given the shape of tracer breakthrough curves (i.e., gradual decrease in concentrations).

8.3 Tracer ERT Monitoring

The site-specific ERT characterization and coupled F&T-ERT evaluations provided several important results that were used to refine the initial tracer test configuration and assess the feasibility of ERT for monitoring a potential ionic tracer test at the 100-H study area.

8.3.1 Site-Specific ERT Characterization

Collecting site-specific ERT images proved to be a very important first step in the evaluation. Images from multiple ERT survey lines indicated numerous high-electrical conductivity features, interpreted as buried metallic infrastructure (e.g., pipelines, reinforced concrete footings, and basin floors) associated with the partially decommissioned remnants of the former 126-H-2 Clearwell Facility and 183-H Solar Evaporation Basin (Figure 3.2 and Figure 3.3). Accordingly, well 199-H3-13 was selected as the injection well for a the forced-gradient tracer test with capture by extraction well 199-H3-22 (Figure 2.3).

8.3.2 Tracer Concentration and Volume Requirements

Results from the numerical F&T model were incorporated into ERT imaging simulations (Figure 5.1) and used to evaluate the ability of ERT to spatially resolve different Br tracer volumes and concentrations. Results suggest that time-lapse ERT can spatially resolve the tracer location during transport from the injection well to the extraction well. However, injection concentrations ≥ 30 g/L and volumes $\geq 10,000$ gallons may be required (Figure 5.2 and Figure 5.4).

8.3.3 Transport Estimates

Spatial moment analysis of the time-lapse ERT images has the potential to be used to calculate the coordinates of the tracer's 2D center of mass and transport velocity through time. The accuracy of these estimates will depend on ERT imaging to spatially resolve the tracer accurately. Again, injection volume and concentrations will need to be sufficiently large to support these calculations (see above). Even if ERT is unable to provide robust quantitative estimates of tracer velocity due to ERT resolution limitations, this information still provides another valuable line of qualitative evidence of tracer transport that can aid in the quantitative interpretation of the extraction well breakthrough curves. It is unlikely ERT imaging can be used to quantify estimates of dispersivity (longitudinal or transverse) given these imaging limitations. However, it may help identify preferential flow paths or other understand non-ideal flow and transport conditions, which would not be distinguishable from a traditional analysis of extraction well breakthrough curves.

8.3.4 Recommended ERT Collection

The results of the evaluation provide an expectation that time-lapse ERT can spatially resolve the tracer transport for injection concentrations and volumes ≥ 30 g/L and $\geq 10,000$ gallons, respectively (see above). Results are less encouraging for ERT imaging at a lower concentrations or volumes (e.g., 10 g/L at 10,000 gallons). However, it is possible that time-lapse ERT imaging of the field tracer will result in better-than-predicted image resolution. ERT provides another line of evidence to aid in the tracer test analysis (discussed above), and this value outweighs the minimal financial cost and schedule impact associated with the ERT field data collection. For these reasons, it is recommended that an ERT array, similar to lines 1b and 2 shown in Figure 3.1, be initially installed and used to monitor transport of a potential Br tracer test, and removed if results indicate tracer transport cannot be observed.

9.0 Conceptual Tracer Test Design

This section describes the conceptual design for a potential tracer test in the RUM aquifer based on an integration of the test objectives, key considerations and constraints, and the results from the comprehensive evaluation presented in the preceding sections (Table 9.1).

Note this is intended to provide a high-level overview of the test configuration for go/no-go determination and planning of subsequent activities. If and when a determination to proceed with field implementation is made, additional field test instruction documents will be generated to detail the step-by-step field testing and monitoring procedures, data requirements, and specific areas of coordination and support by the site contractor. Similarly, environmental health and safety reviews, approvals, and related permitting will need to take place prior to field testing.

Table 9.1. Conceptual tracer design recommendations for a potential bromide tracer test in the uppermost RUM aquifer in the 100-H Area

Design Element or Test Parameter	Value	Comment
Tracer test type	Forced-gradient (convergent flow)	
Injection well	199-H3-13	Will require intermittent well access from 1 month prior to injection to end of test. Pacific Northwest National Laboratory (PNNL) will coordinate with site contractor to ensure routine groundwater sampling by site contractor is not impeded.
Extraction well	199-H3-22	Extraction well 199-H3-29 is also nearby, but results indicate the tracer will be captured solely by 199-H3-22 due to its higher flow rate and closer proximity to the injection well.
Tracer composition	Potassium bromide (KBr)	
Target injection volume	10,000 gal	
Target injection concentration	10 g/L KBr	
Expected peak tracer arrival at extraction well	~100 days	
Expected peak tracer concentration in extraction well	~100 mg/L	About 100x decrease from injected to extracted concentration.
Expected blended concentration in HX P&T facility	<10 mg/L	Influent = effluent Br concentration. This was a primary design consideration to keep effluent as low as possible to minimize mass of Br injected into aquifer through the HX P&T injection wells. Blending ratio of ~15:1 is expected based on typical flow rate of well 199-H3-22 relative to total influent flow rate (see Section 6.0).
Total test duration	6 months	Time to near-zero Br in extraction well

Design Element or Test Parameter	Value	Comment
Target injection start month	March 2022	Peak concentrations are likely to occur during higher-water-table conditions, which will maintain or increase blending (decreased tracer concentration) by other P&T wells. Injection will require 1-2 days, with setup several weeks prior and takedown a week following injection.
Expected monitoring end month	September 2022	
P&T flow rates requirements	As continuous and constant as possible	Decreases or interruptions in flow in well 199-H3-22 by P&T operations may result in increased tracer test duration.
Groundwater sampling in extraction well	1x per week, collected at HX transfer building by Central Plateau Cleanup Company samplers	Samples delivered to PNNL (331 Building).

10.0 Quality Assurance

This work was performed in accordance with the PNNL Nuclear Quality Assurance Program (NQAP). The NQAP complies with the DOE Order 414.1D, *Quality Assurance*. The NQAP uses NQA-1-2012, *Quality Assurance Requirements for Nuclear Facility Application* as its consensus standard and NQA-1-2012 Subpart 4.2.1 as the basis for its graded approach to quality.

11.0 References

- Archie GE. 1942. "The Electrical Resistivity Log as an Aid in Determining Some Reservoir Characteristics." *Transactions of the AIME* 146(01):54-62. Paper no. SPE-942054-G.
doi:10.2118/942054-G
- ASME NQA-1-2012, *Quality Assurance Requirements for Nuclear Facility Application*. American Society of Mechanical Engineers, New York, NY.
- Budge TJ. 2020. *Model Package Report: Plateau to River Groundwater Model, Version 8.3*. CH2M Hill Plateau Remediation Company, Richland, WA.
- Cole CR, MP Bergeron, CJ Murray, PD Thorne, SK Wurstner, and PM Rogers. 2001. *Uncertainty Analysis Framework – Hanford Site-Wide Groundwater Flow and Transport Model*. PNNL-13641, Pacific Northwest National Laboratory, Richland, WA.
- Cohen RM, AH Vincent, JW Mercer, CR Faust, and CP Spalding. 1994. *Methods for Monitoring Pump-and-Treat Performance*. EPA/600/R-94/123, U.S. Environmental Protection Agency, Office of Research and Development, R.S. Kerr Environmental Research Laboratory, Ada, OK.
- Dafflon B, W Barrash, M Cardiff, and T C Johnson. 2011. "Hydrological Parameter Estimations from a Conservative Tracer Test with Variable-Density Effects at the Boise Hydrogeophysical Research Site." *Water Resources Research* 47:1-19.
- Davis SN, GM Thompson, HW Bentley, and G Stiles. 1980. "Ground-water Tracers – A Short Review." *Ground Water* 18(1):14-23.
- DOE Order 414.1D, Quality Assurance. U.S. Department of Energy, Washington, D.C.
- DOE, Ecology, and EPA. 2018. *Record of Decision Hanford 100 Area Superfund Site 100-DR-1, 100-DR-2, 100-HR-1, 100-HR-2, and 100-HR-3 Operable Units*. U.S. Department of Energy, U.S. Environmental Protection Agency (Region 10), and Washington State Department of Ecology, Olympia, WA. <https://pdw.hanford.gov/arpir/index.cfm/viewDoc?accession=0065047H>.
- DOE/RL-96-61. 1997. *Hanford Site Background: Part 3, Groundwater Background*. Rev. 0, U.S. Department of Energy, Richland Operations Office, Richland, WA.
- DOE/RL-2010-95. 2014. *Remedial Investigation/Feasibility Study for the 100-DR-1, 100-DR-2, 100-HR-1, 100-HR-2, and 100-HR-3 Operable Units*. Rev. 0, U.S. Department of Energy, Richland Operations Office, Richland, WA.
- DOE/RL-2017-13. 2020. *Remedial Design/Remedial Action Work Plan for the 100-DR-1, 100-DR-2, 100-HR-1, 100-HR-2, and 100-HR-3 Operable Units*. Rev. 0, U.S. Department of Energy, Richland Operations Office, Richland, WA.
- DOE/RL-2019-66. 2020. *Hanford Site Groundwater Monitoring Report for 2019*. Rev. 0, U.S. Department of Energy, Richland Operations Office, Richland, WA.

- DOE/RL-2019-67. 2020. *Calendar Year 2019 Annual Summary Report for the 100-HR-3 and 100-KR-4 Pump and Treat Operations, and 100-NR-2 Groundwater Remediation*. Rev. 0, U.S. Department of Energy, Richland Operations Office, Richland, WA.
- Fang Y, D Appriou, DH Bacon, V Freedman, ML Rockhold, C Ruprecht, G Tartakovsky, MD White, SK White, and F Zhang. 2018. *eSTOMP Online User Guide*. Pacific Northwest National Laboratory, Richland, WA. http://stomp.pnnl.gov/estomp_guide/eSTOMP_guide.stm.
- Fayer MJ and TB Walters. 1995. *Estimated Recharge Rates at the Hanford Site*. PNL-10285, Pacific Northwest Laboratory, Richland, WA.
- Isono T. 1984. "Density, Viscosity, and Electrolytic Conductivity of Concentrated Aqueous Electrolyte Solutions at Several Temperatures. Alkaline-Earth Chlorides, LaCl_3 , Na_2SC_4 , NaN_3 , NaBr , KNC_3 , KBr , and $\text{Cd}(\text{NO}_3)_2$." *Journal of Chemical and Engineering Data* 29(1):45-52.
- Istok JD and MD Humphrey. 1995. "Laboratory investigation of buoyancy-induced flow (plume sinking) during 2-well tracer tests." *Ground Water* 33(4), 597-604.
- Johnson TC, GE Hammond, and X Chen. 2017. "PFLOTRAN-E4D: A parallel open source PFLOTRAN module for simulating time-lapse electrical resistivity data." *Computers & Geosciences* 99:72-80. <https://doi.org/10.1016/j.cageo.2016.09.006>
- Johnson TC and DM Wellman. 2013. *Re-inversion of surface electrical resistivity tomography data from the Hanford Site B-Complex*. PNNL-22520, Pacific Northwest National Laboratory, Richland, WA.
- Johnson TC and D Wellman. 2015. "Accurate modelling and inversion of electrical resistivity data in the presence of metallic infrastructure with known location and dimension." *Geophysical Journal International* 202(2):1096-1108.
- Kim JW. 2014. "Optimal pumping time for a pump-and-treat determined from radial convergent tracer tests." *Geosciences Journal* 18:69-80.
- Mackley RD, V Garayburu-Caruso, VL Freedman, and KM Engbrecht. 2020. *Hydrologic Evaluation of the Ringold Upper Mud Aquifer in the 100-H Area of the Hanford Site*. PNNL-30467, Pacific Northwest National Laboratory, Richland, WA.
- Maliva RG. 2016. *Aquifer Characterization Techniques*, Chapter 13, "Tracer Tests." Springer International Publishing, Basel, Switzerland.
- Robinson J, RD Mackley, ML Rockhold, TC Johnson, and P Jaysaval. 2020. *Geophysical Methods for Stratigraphic Identification*. PNNL 29182, Rev. 1, Pacific Northwest National Laboratory, Richland, WA.
- SGW-46279. 2016. *Conceptual Framework and Numerical Implementation of 100 Areas Groundwater Flow and Transport Model*. Rev. 3, CH2M Hill Plateau Remediation Company, Richland, WA. <https://pdw.hanford.gov/document/0076173H>
- SGW-60571. 2017. *Aquifer Testing of the First Water-Bearing Unit in the RUM at 100-H*. Rev. 0, CH2M Hill Plateau Remediation Company, Richland, WA.

Singha K, FD Day-Lewis, T Johnson, and LD Slater. 2015. "Advances in interpretation of subsurface processes with time-lapse electrical imaging." *Hydrological Processes* 29(6):1549-1576.

Singha K and SM Gorelick. 2005. "Saline tracer visualized with three-dimensional electrical resistivity tomography: Field-scale spatial moment analysis." *Water Resources Research* 41:1-17.
<https://doi.org/10.1029/2004WR003460>

Truex MJ, VR Vermeul, BG Fritz, RD Mackley, DP Mendoza, RP Elmore, AV Mitroshkov, DS Sklarew, CD Johnson, M Oostrom, DR Newcomer, FJ Brockman, CL Bilskis, SS Hubbard, JE Peterson, KH Williams, E Gasperikova, and J Ajo-Franklin. 2009. *Hanford 100-D Area Biostimulation Treatability Test Results*. PNNL-18784, Pacific Northwest National Laboratory, Richland, WA.

Vermeul VR, BN Bjornstad, BG Fritz, JS Fruchter, RD Mackley, DP Mendoza, DR Newcomer, ML Rockhold, DM Wellman, and MD Williams. 2009. *300 Area Uranium Stabilization through Polyphosphate Injection: Final Report*. PNNL-18529, Pacific Northwest National Laboratory, Richland, WA.

Williams MD, VR Vermeul, JE Szecsody, and JS Fruchter. 2000. *100-D Area In Situ Redox Treatability Test for Chromate-Contaminated Groundwater*. PNNL-13349, Pacific Northwest National Laboratory, Richland, WA.

Williams MD, BG Fritz, DP Mendoza, ML Rockhold, PD Thorne, YL Xie, BN Bjornstad, RD Mackley, JE Szecsody, and VR Vermeul (2008). *100-NR-2 Apatite Treatability Test: Low Concentration Calcium Citrate-Phosphate Solution Injection for In Situ Strontium-90 Immobilization*. PNNL-17429, Pacific Northwest National Laboratory, Richland, WA.

Appendix A – Laboratory Batch Tests

This appendix describes the methods and results for laboratory batch testing evaluations of potential Br impacts to the SIR-700 ion exchange resin performance for treating Cr(VI).

A.1 Methodology

A set of batch tests were conducted using the SIR-700 resin to provide an indication of the effect of Br on Cr treatment by the SIR-700 resin. The experimental design for the batch testing included the following variables:

- a. Type of resin to be tested: SIR-700
- b. Br concentrations (four: 0, 100, 1000, 30,000 mg/L)
- c. Cr concentrations (four: 0, 25, 100, 250 µg/L)
- d. Time (four: 1 hour, 12 hours, 1 day, and 7 days)
- e. Replicates: two
- f. Controls: One for each spiked solution with no resin present (a total of 16)

The resin was pre-treated prior of use to remove any residual metals or anions left over from the manufacturing process by centrifuge washing two times for 1 hour with double deionized (DDI) water at a solution-to-solid ratio of 3:1, followed by centrifugation at 1700 rpm for 5 minutes. After decanting the second wash water, the resin was put in container with DDI water for 24 hours. The excess water was removed after 1 day and the resin was dried at room temperature until the start of the tests. The moisture content was measured in the resin to calculate the mass of resin added in each batch reactor.

In the batch adsorption tests, Br and Cr spiked solutions were prepared by adding the appropriate amount of KBr and sodium chromate to a synthetic ground water (SGW) to obtain the concentrations included in the experimental design. The SGW was made by addition of the reagents to DDI water in the order identified in Table A.1. To prepare the synthetic groundwater, we initially dissolved silicic acid and subsequently added other ingredients. The pH was adjusted by stirring and the final pH was about 8.0. The silicic acid dissolves slowly, causing the pH to slowly decrease.

Table A.1. Synthetic Hanford groundwater recipe [from Jim Szecsody (BNW54773:62-63), Nov. 6, 2002 (BNW56964:78)].

Constituent	Concentration (mg/L)	Amount to add to 2 L (mg)
H ₂ SiO ₃ *nH ₂ O, silicic acid	15.3	30.6
KCl, potassium chloride	8.20	16.4
MgCO ₃ , magnesium carbonate	13.0	26.0
NaCl, sodium chloride	15.0	30.0
CaSO ₄ , calcium sulfate	67.0	134
CaCO ₃ , calcium carbonate	150	300

For these batch loading tests, SIR-700 resin and the SGW solution containing dissolved Br and Cr were combined at a 1:10 ratio and were placed into a 50-mL centrifuge tube (1 g of resin and 10 mL of contacting solution). Process blanks included solution blanks (initial Br and Cr solutions with no material) and a material blank (material in simulated groundwater with no Br and Cr). Process blanks were prepared and handled in the same manner as all other loading tests.

The centrifuge tubes were sealed and placed on a shaker table set at 125 rpm to ensure the resin and Br- and Cr-containing SGW solutions remained well mixed for the duration of the experiments. All loading tests and process blanks were kept at room temperature under aerobic conditions. After the designated elapsed times, the centrifuge tubes were removed from the shaker table and allowed to settle for 15 minutes. The liquid was decanted into a syringe, then filtered with a 0.20- μ m filter to separate the aqueous matrix from the sorbent. A 10-mL aliquot was removed, approximately 5-mL was pushed through the filter to prime the filter, and the remaining solution was placed into a liquid scintillation vial.

Actual material masses and solution volumes used in the batch tests were recorded and all tests were run in duplicate. pH measurements were taken as soon as the resin was exposed to the spiked liquid phase and at the end of experiment after separation of the solid from the liquid.

Total Cr was determined by Inductively coupled plasma mass spectrometry. The detection limit for total Cr was 0.35 μ g/L (prior to dilution). Total Br was determined using a Br selective electrode. Analytes are method-specific and include cations by inductively coupled plasma optical emission spectrometry and anions by ion chromatography.

A.2 Results

As noted above, the batch tests provide an efficient method for evaluating bromide (Br) effects on the SIR-700 resin over many combinations of Br and Cr concentrations. Results shown include only select results where Br or Cr were varied over a range of concentrations while keeping the other constituent at a zero concentration for control. The changes in pH, Br, and Cr concentration over time are presented below (in that order), followed by general conclusions from the batch results.

A.2.1 pH

Aqueous phase pH decreased rapidly for all combinations of Br and Cr in batch reactors (Figure A.1). This is consistent with data provided on resin performance (which is ideal at pH values around 6). In the tests conducted with solutions that contained zero or 100 mg/L Br, the pH decreased rapidly within the first hour from initial values of about pH = 7.5 - 7.8 to pH = 5.5 - 6.0 and did not change during the course of the tests (1 day). However, in the tests conducted with 1000 and 30,000 mg/L Br, the pH decreased much less and equilibrated to pH ~6.5 and pH ~7.3, respectively. The pH remained unchanged for the duration of these tests (i.e., 1 day) (Figure A.1). A similar effect on pH was not observed in the tests conducted with increasing Cr concentrations (in the absence of Br), most likely because the Cr concentrations used in these tests were low (e.g., 0, 25, 100, and 250 μ g/L, Figure A.2), consistent with concentrations at the site.

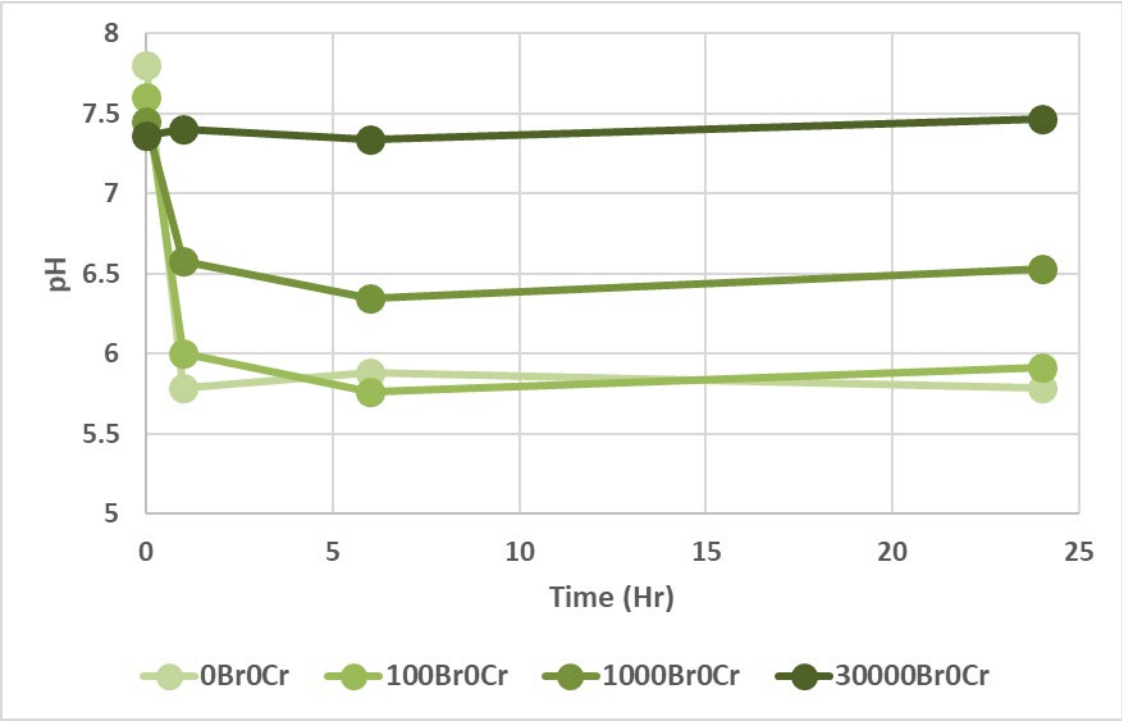


Figure A.1. pH changes during the first day of the batch testing with varying bromide concentrations and zero Cr.

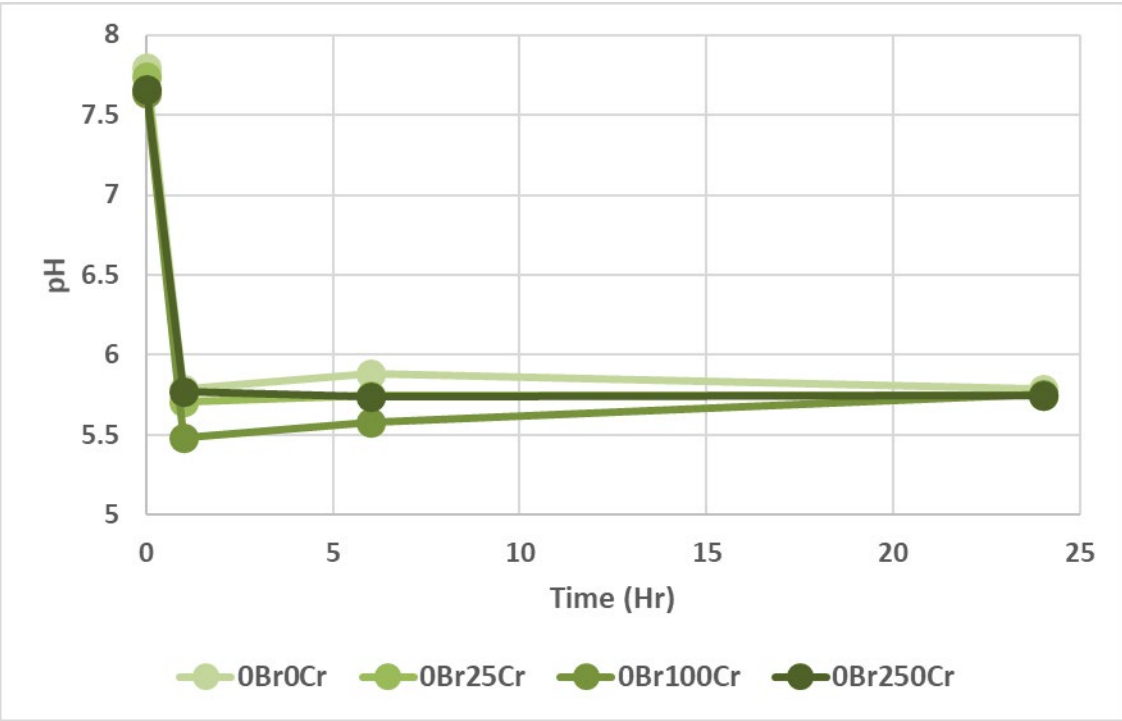


Figure A.2. pH changes during the first day of the batch testing with varying chromate concentrations and zero Br.

A.2.2 Bromide

Bromide concentrations decreased rapidly and significantly but Br was not completely removed from the aqueous phase by the resin. In the tests conducted with initial Br concentrations of 100, 1000, and 30,000 mg/L, the concentration decreased rapidly in the first hour and changed slightly in first day of the experiments (Figure A.2). In the test conducted with the 30,000 mg/L Br concentration, the aqueous concentrations showed a slight increase toward the end of the 7-day period (Figure A.3). This unexpected resin behavior could be related to the resin's sorption capacity or breakdown/fouling of the resin by the high Br (salt) load.

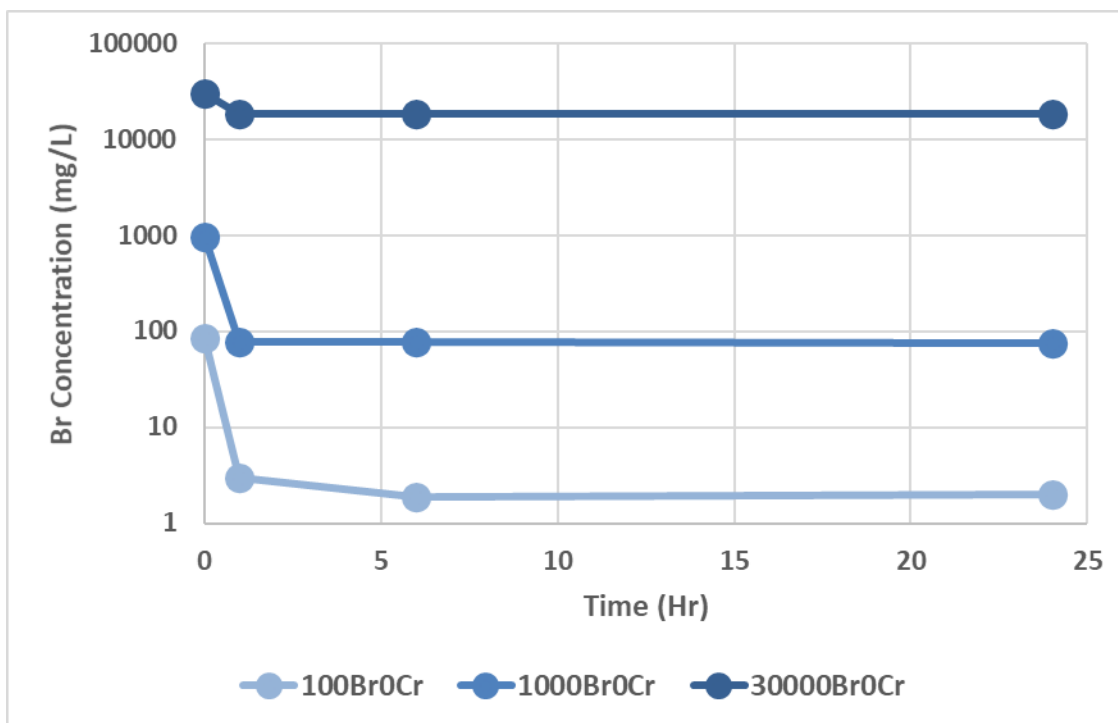


Figure A.3. Bromide concentrations for the first 24 hours of batch testing at varying initial bromide concentrations and zero Cr.

A.2.3 Chromate

Chromate concentrations decreased below 10 $\mu\text{g/L}$ within 24 hours for the 100 mg/L and 1000 mg/L Br batches (Figure A.4). The 30,000 mg/L Br and 250 $\mu\text{g/L}$ Cr treatment reached a Cr concentration of about 4 $\mu\text{g/L}$ after 7 days (Figure A.3). The trends of decreased chromate concentration in the batch tests generally mirror the trends of decreased Br concentrations through time (Figure A.2).

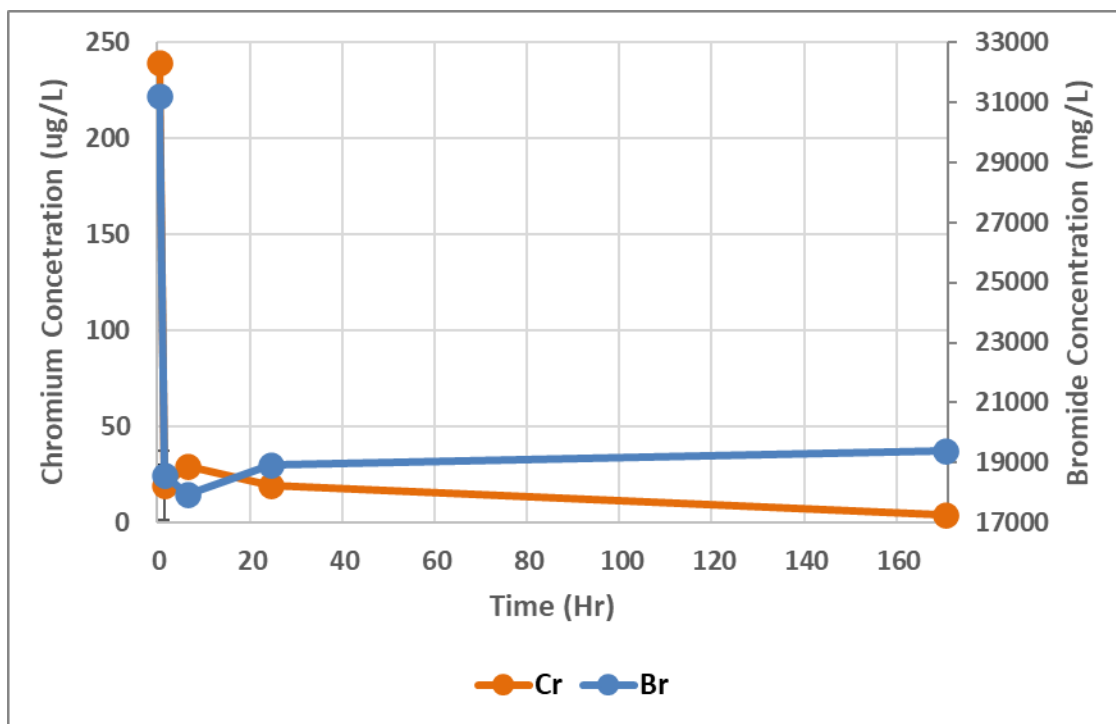


Figure A.4. Bromide (blue) and chromate (orange) concentrations over the 7-day (168-hour) batch testing at initial bromide and chromate concentrations of 30,000 mg/L and 250 $\mu\text{g/L}$ chromate, respectively.

A.2.4 General Conclusions

The following general conclusions can be made from the batch experiments:

1. Increased Br concentrations (equal or greater than 1000 mg/L) may impact resin performance as demonstrated by the increased concentration in aqueous Cr when exposed to 30,000 mg/L Br and the significant changes in pH values measured in the batch experiments.
2. The removal of aqueous Br following exposure to the resin suggests important interactions between Br and the resin. Partial aqueous Br removal, especially the release of Br back into solution with time, indicates unusual resin performance that requires further testing.
3. Br concentrations up to 1000 mg/L do not influence chromate removal at Cr concentrations tested in these experiments (e.g., 0 to 250 $\mu\text{g/L}$). However, at 30,000 mg/L Br, Cr removal by the resin is less effective, especially initially, and the observed trends are difficult to understand. Data suggests competition between Br and Cr, resulting initially in less Cr removal and demonstrating the resin's inability to remove sufficient amount of Cr to achieve a concentration of 10 $\mu\text{g/L}$ or less. Future test should determine the time-dependent Cr removal in flow through experiments, under similar conditions.

Pacific Northwest National Laboratory

902 Battelle Boulevard
P.O. Box 999
Richland, WA 99354
1-888-375-PNNL (7665)

www.pnnl.gov